Org Divers Evol (2015) 15:1–21
DOI 10.1007/s13127-014-0183-5

ORIGINAL ARTICLE

ORGANISMS DIVERSITY & EVOLUTION

Description of a new syllid species as a model for evolutionary research of reproduction and regeneration in annelids

María Teresa Aguado · Conrad Helm · Michael Weidhase · Christoph Bleidorn

Received: 30 May 2014 / Accepted: 12 September 2014 / Published online: 5 October 2014

Abstract Syllids are one of the most speciose annelid taxa and characterized by their variety of reproductive modes. We provide the description of a new species of Syllidae (Annelida, Phyllodocida), *Typosyllis antoni* n. sp., which is characterized by its distinct color pattern consisting of transversal red lines on the dorsum of anterior segments; long antennae and dorsal cirri with strong alternation in length; bidentate chaetae falciger like with long spinulation on edge, one tiny and thin acicula appearing in posterior segments in addition to thicker and pointed one, and a long proventricle. A phylogenetic analysis of Syllinae based on three genes supports that *T. antoni* n. sp. is sister species to *Typosyllis heronislandensis*. This sister group relationship may indicate a common ancestor from the Pacific. Moreover, we recommend several steps to unify the taxonomy with phylogenetic knowledge of this group. Using immunocytochemistry coupled with confocal laser scanning microscopy (cLSM), we describe the internal morphology of this species. The body wall is composed of two dorsal and two ventral longitudinal muscle bundles that form a distinct inner layer. The outer or "circular layer" of body wall musculature is represented by prominent transverse muscle fibers that exhibit a semicircular arrangement. The musculature of the uniramous parapodia is characterized by distinct parapodial retractor muscles, acicular protractor muscles, as well as prominent acicular and chaetal flexor muscle bundles. *T. antoni* n. sp. reproduces by schizogamic scissiparity producing dicerous stolons. This species is able to regenerate the anterior end, including the prostomium, the first chaetae-less segment with all appendages, and some additional chaetigers, depending on the dissection side. Regeneration of the proventricle, ventricle, caeca, or pharyngeal tooth is not detectable. In contrast, regeneration of the posterior end appears to be complete. The available data makes *T. antoni* n. sp. to be one of the best investigated syllids, emphasizing its potential as model for the whole group. Our analysis establishes a framework for future studies on the evolution of reproductive modes in Syllidae, and we outline research questions how they are related to regeneration and development.

Keywords Annelida · cLSM · Development · Musculature · Polychaetes · Regeneration · Reproduction · Syllidae

M. T. Aguado (✉)
Departamento de Biología, Facultad de Ciencias, Universidad Autónoma de Madrid, Cantoblanco, 28049 Madrid, Spain
e-mail: maite.aguado@uam.es

C. Helm · M. Weidhase · C. Bleidorn
Molecular Evolution and Systematics of Animals, Institute of Biology, University of Leipzig, Talstraße 33, D-04103 Leipzig, Germany

C. Helm
e-mail: helm@uni-leipzig.de

M. Weidhase
e-mail: michael.weidhase@uni-leipzig.de

C. Bleidorn
e-mail: bleidorn@uni-leipzig.de

Introduction

Recent advances in morphological and molecular techniques enabled the toolkit for evolutionary research in non-model invertebrates to be expanded. For annelids (and lophotrochozoans in general), *Platynereis dumerilii* became a model to investigate questions related to the evolution of organ systems, circadian clocks, and early development (Simakov et al. 2013). Many of these studies are only accomplishable due to the fact that *P. dumerilii's* life cycle is well known, and it can be kept under controlled laboratory conditions (Fischer and Dorresteijn 2004). Moreover, many techniques known from *Drosophila* and *Caenorhabditis* research

are established for these animals (transgenic lineages, morpholino knockdowns, RNA interference), and new approaches have been developed (Zantke et al. 2014). However, only few other annelids became focus of such an intensive research program and most evolutionary lineages of this hyperdiverse animal phylum are neglected. One such example is the family Syllidae.

Within Annelida, the Syllidae are one of the most speciose and taxonomically complex groups. Currently, there are 74 genera and nearly 700 valid species (Aguado and San Martín 2009; Aguado et al. 2012). Syllidae are of high interest from an evolutionary point of view due to their variety of sexual reproductive modes, which can be principally distinguished into epigamy and schizogamy (Franke 1999; Nygren 1999). Some species such as *Ramisyllis multicaudata* show such a derived pattern of these modes that they evolved branching animals, which has not been reported for any other annelid so far (Glasby et al. 2012). Other species form long chains of animals due to stolonization (e.g., *Myrianida* sp.), and for some syllids, a highly complex mating behavior involving dancing or bioluminescent displays are described (Franke 1999; Fischer and Fischer 1995). However, only few attempts have been made to unravel the genetic and morphological adaptations to facilitate these complex reproductive modes.

Syllidae are usually small in size and their taxonomic characteristics are mostly related to details of chaetae shape and spinulation. Syllids are identified easily at family level because they all show a differentiation of their digestive tube, the so-called proventricle. This structure is supposed to act as a suctorial pump during the feeding process (Fauchald and Jumars 1979; Heacox and Schroeder 1982; Franke 1983, 1986) and has been proposed to be the autapomorphy of the group (Glasby 2000; Pleijel 2001; Aguado et al. 2007, 2012; Aguado and San Martín 2009).

Recently, Aguado et al. (2012) performed the most inclusive phylogenetic study (more than 300 terminals), including morphology and DNA, to discuss and revise the systematics of Syllidae. According to this study, the family is divided into different evolutionary lineages: the subfamilies Anoplosyllinae, Autolytinae, Exogoninae, Eusyllinae, and Syllinae, as well as some genera grouping outside these taxa. Aguado et al. (2012) also showed that several genera might not be monophyletic and in need of revision. The subfamily Syllinae is the largest one, with the highest number of taxa (20 genera and about 260 species), and also the most conflictive group in terms of systematics, since most of its genera are either paraphyletic or polyphyletic (Aguado et al. 2012).

Syllis-Typosyllis is the largest group within Syllidae, including more than 130 species (Licher 1999; San Martín 2003). Licher (1999) made an extensive and thorough revision of *Typosyllis* (sensu Licher 1999), organizing the species in different complexes. However, this group is highly diverse, and descriptions of new species have increased since then. *Syllis* Lamarck, 1818, is the type genus of the family (Lamarck 1818); it was divided by Langerhans (1879) in four subgenera attending solely based on chaetal characters: *Typosyllis* Langerhans, 1818, with compound chaetae, all with falcigers blades (short length); *Ehlersia* Quatrefages, 1865, with compound chaetae and some elongated spiniger-like blades (long length) in some parapodia; *Haplosyllis* Langerhans, 1879, with only simple chaetae; and *Syllis*, with falcigers and thick simple chaetae on some parapodia, produced by lose of blades and enlargement of shafts or by blades and shafts fused (see Fig. 10, Licher 1999).

However, the fusion of shafts and blades occurs while specimens grow; therefore, the same species can have fused chaetae or not, depending on the size. Additionally, there are some species for which the fusion process never completes; they show partially or incompletely fused shafts and blades, in which the blade and shaft can be recognized (Aguado et al. 2008). Not surprisingly, the conflictive systematics of the *Syllis-Typosyllis* group was revealed by recent phylogenetic analyses (Aguado et al. 2007; Aguado et al. 2012). Consequently, Aguado et al. (2012) proposed to use *Syllis* or *Typosyllis* generic assignation depending on the original description, until more phylogenetic information is provided and this conundrum can finally be solved.

In this study, a new species of this complex group, *Typosyllis antoni* n. sp., is described. We provide a large amount of information available obtained through multiple methodologies. Different techniques to study external morphology (light microscopy and scanning electron microscopy (SEM)), internal anatomy (confocal laser scanning microscopy (cLSM)), as well as a phylogenetic background are, by the first time, used in combination in the most complete description of a new species of Syllidae. Moreover, we describe reproductive stages and regeneration experiments for this new species. Together, this provides a framework for future evolutionary research of this diverse group of syllids.

Material and methods

All specimens of *T. antoni* n. sp. were collected in the aquarium facility of the University of Leipzig. The animals lived in coarse sediment at a salinity of 3.6 %, and the aquaria had a temperature of 24–29 °C. The access to living animals enabled different kinds of studies regarding morphological features developed at different stages of the life cycle (i.e., stolonization, regeneration).

The type series is deposited at the Museo Nacional de Ciencias Naturales de Madrid (MNCN); additional material is deposited at the Institute of Biology, University of Leipzig (UL). Other examined material for DNA sequencing belongs to the collections of the Australian Museum (AM);

comparative material examined belongs to the Zoologischen Museum Hamburg (ZMH).

Light microscopy and SEM

Samples for light microscopical studies were fixed in 10 % formaldehyde-seawater solution and preserved in 70 % alcohol solution. Specimens for DNA extraction were fixed directly in 90 % ethanol. Some specimens were stained with methylene blue to observe glands and other features. All observations were made using a compound microscope with interference contrast optics (Nomarsky). Olympus SZ30 stereomicroscope and Olympus CH30 optic microscope were subsequently used for identification. Light microscopic pictures were taken by using a Leica (Leica Microsystems, Wetzlar, Germany) DM1000 microscope with a Leica DFC295 camera and the Leica LAS V3.6 software. Final drawings and image plates were designed by using Adobe (San Jose, CA, USA) Photoshop CS6 and Illustrator CS6. Paratypes (MNCN 16.01/15469-71) were critical point dried and subsequently coated with 102 Å of gold for scanning electron micrographs. Specimens were examined with a scanning electron microscope (SEM) Philips FEI INSPECT (Hillsboro, Oregon, USA) at the Museo Nacional de Ciencias Naturales de Madrid (MNCN, CSIC). Width of the specimens is measured at level of the proventricle, without parapodia.

Regeneration study

Regeneration experiments were performed at the University of Leipzig during May 2014. Specimens without signs of gametogenesis or stolonization were anesthetized in 3.5 % $MgCl_2$ in artificial seawater and dissected between chaetiger 35 and 36 by using a scalpel. The cutting site was chosen to ensure the removal of the proventricle, the ventricle, and the caeca and corresponds to a division in one and two thirds of the body. Subsequently, the anterior and posterior ends were placed in separate plastic bowls, each filled with 0.5 l artificial seawater, a small amount of coral grit, and an air influx. Specimens were kept without feeding at a temperature of 25 ±1 °C. To simplify the fixation of specimens every day, two distinct experimental series were performed with a time shift of 4 days. A fifth plastic bowl was set up with six control specimens, which were treated like described above, but without dissection. Altogether, 48 specimens were used for the experiments. Every day after dissection, three anterior and three posterior regenerating specimens were removed, anesthetized in 7 % $MgCl_2$ in artificial seawater and fixated in 4 % paraformaldehyde (PFA) in 0.1 M phosphate-buffered saline (PBS, pH 7.4) overnight at 4 °C. Afterwards, the probes were rinsed in 0.1 M PBS for at least 3 h and stored in 0.1 M PBS including 0.05 % NaN_3 at 4 °C until usage.

Immunocytochemistry and cLSM

Several specimens were fixed using 4 % PFA in 0.1 M PBS (pH 7.4) overnight at 4 °C. Afterwards, specimens were washed for at least 3 h in 0.1 M PBS and stored in 0.1 M PBS including 0.05 % NaN_3 at 4 °C until usage. Two different stainings were used: anti-F-actin staining and anti-serotonin immunolocalization.

Anti-F-actin staining was used to stain muscle tissue. Specimens were pre-incubated for 2×60 min in 0.1 M PBS and subsequently incubated in a solution containing phalloidin–rhodamine (5 μl methanolic stock solution in 500 μl PBS; Invitrogen, Darmstadt, Germany). Subsequently, specimens were dehydrated in an ascending isopropanol series, treated in Murray's clearing solution (benzyl alcohol plus benzyl benzoate, 1:2) and mounted between two coverslips in dibutyl phthalate xylene (DPX) (Sigma-Aldrich, St. Louis, MO, USA).

For anti-serotonin staining, antibody staining was preceded by tissue permeabilization for 1 h in 0.1 M PBS containing 0.1 % NaN_3 and 0.1 % Triton X-100 (PTA), and suited by incubation in block-PTA (6 % normal goat serum (Sigma-Aldrich, St. Louis, MO, USA) overnight. The primary antibody polyclonal rabbit anti-serotonin (INCSTAR, Stillwater, MN, USA, dilution 1:500) was applied for 48–72 h in block-PTA. Afterwards, specimens were rinsed in block-PTA for 3× 2 h and incubated subsequently with a secondary fluorochrome conjugated antibody (goat anti-rabbit Alexa Fluor 488, Invitrogen, Carlsbad, CA, USA, dilution 1:500) in block-PTA for 24–48 h. At last, the specimens were washed three times in 0.1 M PBS (without NaN_3). Subsequently, specimens were dehydrated in an ascending isopropanol series, treated in Murray's clearing solution (benzyl alcohol plus benzyl benzoate, 1:2) and mounted between two coverslips in DPX (Sigma-Aldrich, St. Louis, MO, USA). For additional muscle staining, the last washing step was performed as described for the anti-F-actin staining. Negative controls were obtained by omitting the primary antibody in order to check for antibody specificity and yielded no fluorescence signal.

Specimens were analyzed with the confocal laser scanning microscope Leica TCS STED (Leica Microsystems, Wetzlar, Germany). Confocal image stacks were processed with Leica AS AF v2.3.5 (Leica Microsystems) and Imaris 6.3.1 (Bitplane AG, Zurich, Switzerland).

Phylogenetic study

Sequences of the nuclear 18S gene and two mitochondrial genes (16S and COI) were downloaded from GenBank for syllid and outgroup species (Table 1). To obtain the sequences for additional syllid species for these three genes, DNA extraction, primers, purification, amplification, and sequencing procedures were applied as in Aguado et al. (2007, 2012).

Table 1 Terminals used in the analyses, sampling sites, and GenBank accession numbers

	Sample site	18S	16S	COI
Ingroup				
Amblyosyllis madeirensis	San Esteban, Asturias, Spain	JF903574	JF903683	JF903774
Branchiosyllis cirropunctata	Green Head, WA, Australia	JF903580	JF903690	
Branchiosyllis exilis 1	Darwin, NT, Australia	JF903583	JF903692	
B. exilis 2	Shark Bay, WA, Australia	JF903581-2	JF903691	JF903783
B. exilis 3	Coconut Is., Hawaii, USA	JF903584	JF903693	
Branchiosyllis maculata	Heron Island, QLD, Australia	JF903585	JF903694	
Branchiosyllis sp.	La Jolla, California, USA	AF474283		
Branchiosyllis thylacine	Port Jackson, NSW, Australia	JF903586	JF913951	
Eurisyllis tuberculata 1	Shark Bay, WA, Australia	JF903594		JF903787
E. tuberculata 2	Banyuls-sur-mer, France	EF123833		EF123748
Eusyllis blomstrandi	Kaldbak, Faroe Islands	EF123887	EF123788	EF123749
Haplosyllis cf. *spongicola*	Port Jackson, NSW, Australia	JF903611		
Haplosyllis sp. 1	Shark Bay, WA, Australia	JF903607	JF903698	
Haplosyllis sp. 2	Goodes Is., QLD, Australia	JF903608-9	JF913953	
Haplosyllis sp. 3	Coconut Is., Hawaii, USA	JF903610		
Haplosyllis spongicola 1	Banyuls-sur-mer, France	EF123837	EF123791	EF123751
H. spongicola 2	GenBank	AF474291		
Megasyllis sp. 1	Manazuru, Japan	JF903577	JF903687	
Megasyllis sp. 2	Manazuru, Japan	JF903614		
Megasyllis multiannulata 1	Manazuru, Japan	JF903612	JF903699	
M. multiannulata 2	Manazuru, Japan		JF903700	
Megasyllis nipponica	Manazuru, Japan		EF123813	EF123782
Megasyllis glandulosa	Port Denison, WA, Australia	JF903576	JF903686	
Megasyllis subantennata	Kalbarry, WA, Australia	JF903578	JF903688	JF903775
Megasyllis tigrina	Jervis Bay, NSW, Australia	JF903579	JF903689	
Myrianida convoluta	California, USA	AF474303	AF474257	
Opisthosyllis japonica	Shark Bay, WA, Australia		JF903705	
Opisthosyllis leslieharrisae	California, USA	EF123844		EF123757
Opisthosyllis longocirrata	Heron Island, QLD, Australia	JF903622	JF913959	
Opisthosyllis viridis	Prince of Wales Is., QLD, Aus		JF913960	JF903794
Parahaplosyllis brevicirra	Port Jackson, NSW, Australia	JF903679	JF903706	JF903784
Paraopisthosyllis alternocirra	Rottnest Is., WA, Australia	JF903623	JF903707	JF903786
Paraopisthosyllis cf. *phyllocirra*	Lizard Island, QNLD, Australia	JF903624	JF903708	JF903777
Perkinsyllis augeneri	Sydney, NSW, Australia	EF123832	EF123794	
Perkinsyllis hartmannschroederae	Port Denison, WA, Australia	JF903627		
Perkinsyllis heterochaetosa	Botany Bay, NSW, Australia	JF903628	JF913961	
Perkinsyllis koolalya	Rottnest Is., WA, Australia	JF903629	JF903709	
Pionosyllis enigmatica	Tjärno, Sweden	EF123826	EF123795	EF123758
Prosphaerosyllis battiri	Rottnest Is., WA, Australia	JF903630	JF903711	JF903763
Syllis alternata	Port de la Selva, Girona, Spain	JF903649	JF903726	
Syllis amica	O Grove, Galicia, Spain		EF123821	
Syllis armillaris 1	Kaldbak, Faroe Islands	AF474292		
S. armillaris 2	Cala Ratjada, Mallorca, Spain	JF913969	JF903727	
Syllis augeneri	Port Jackson, NSW, Australia	JF913970		JF903788
Syllis cerina	Prince of Wales Is., QLD, Aus	JF903653	JF903729	
Syllis compacta	Altea, Alicante, Spain	EF123846-7	EF123806	EF123772
Syllis corallicola	Port de la Selva, Girona, Spain	EF123875	EF123807	
Syllis ehlersioides	Manazuru Peninsula, Japan	EF123841	EF123808	EF123773

Table 1 (continued)

	Sample site	18S	16S	COI
Syllis ferrani	Port de la Selva, Girona, Spain	EF123874	EF123809	EF123775
Syllis gracilis 1	O Grove, Galicia, Spain	EF123876	EF123811	EF123778
S. gracilis 2	Prince of Wales Is., QLD, Aus	JF903660	JF903733	JF903778
Syllis cf. *gracilis australiensis* 1	Rat Island, Abroholos, WA, Aus	KM277831		
S. cf. *gracilis australiensis* 2	Cassini, Kimberley, WA, Australia	KM277830		
Syllis hyalina 1	Port de la Selva, Girona, Spain	EF123851-2	EF123818	EF123779
S. hyalina 2	Port Phillip Bay, Victoria, Aus	JF903662	JF903735	
Syllis krohnii	Azores Islands, Portugal	EF123859	EF155920	
Syllis marugani	Manazuru Peninsula, Japan	EF123862-3	EF123812	EF123780
Syllis nigropunctata	Port Jackson, NSW, Australia	JF903664	JF903737	
Syllis okadai	Manazuru Peninsula, Japan	EF123857-8	EF123814	EF123783
Syllis pectinans	Newport, NSW, Australia	JF903666		
Syllis prolifera 1	Cabo de Gata, Almería, Spain	JF903667	JF903739	
S. prolifera 2	Cala Ratjada, Mallorca, Spain	JF903668	JF903740	
Syllis pulvinata	Port de la Selva, Girona, Spain	JF913972	JF903741	
Syllis punctulata	Maroubra, NSW, Australia	JF903669	JF903742	
Syllis variegata	O Grove, Galicia, Spain	JF903670	EF123822	
Syllis cf. *variegata*	Port Jackson, NSW, Australia	JF903655	JF903731	
Syllis vittata	San Esteban Asturias, Spain	JF903671	JF903743	
Syllis vivipara	O Grove, Galicia, Spain	EF123848-9	EF123815	
Syllis westheidei	Port de la Selva, Girona, Spain	EF123877		EF123784
Syllis ypsiloides	Coconut Is. Hawaii, USA	JF903673	JF903745	
Syllis zonata	Port Jackson, New South Wales	JF903674	JF903746	JF903780
Trypanosyllis coeliaca 1	Port de la Selva, Girona, Spain	EF123878	EF123816	EF123785
T. coeliaca 2	Sydney, NSW, Australia	JF903675	JF903749	
Trypanosyllis zebra 1	Prince of Wales Is., QLD, Aus		JF903748	
T. zebra 2	Banyuls-sur-Mer, France	JF903676	EF123817	EF123786
T. zebra 3	Shark Bay, WA, Australia	JF903677	JF903751	
T. zebra 4	Port Jackson,, NSW, Australia	JF903678	JF903752	JF903790
Typosyllis anoculata	GenBank	DQ790098		
Typosyllis antoni n. sp.	Aquarium Leipzig, Germany	SRX513556	SRX513556	SRX513556
Typosyllis bella	Abroholos, WA, Australia	JF913971		JF903779
Typosyllis broomensis	Goodes Is., QLD, Australia	JF903650-1	JF903728	
Typosyllis busseltonensis	Port Jackson, NSW, Australia	JF903652		JF903782
Typosyllis cf. *lutea*	Heron Island, QLD, Australia	JF903654	JF903730	
Typosyllis columbretensis	Port de la Selva, Girona, Spain	JF903656	EF123805	EF123771
Typosyllis crassicirrata	Port Phillip Bay, Victoria, Aus.	JF903657		
Typosyllis edensis	New Port, NSW, Australia	JF903658	JF903732	JF903789
Typosyllis filidentata	Little Kianinny, NSW, Australia	KM277829		
Typosyllis garciai	O Grove, Galicia, Spain	EF123869		EF123776
Typosyllis gerlachi	Port de la Selva, Girona, Spain	JF903659	EF123810	EF123777
Typosyllis heronislandensis	Heron Island, QLD, Australia	JF903661	JF903734	
Typosyllis lutea 1	Sydney, NSW, Australia	EF123865		
T. lutea 2	Shark Bay, WA, Australia	JF903663	JF903736	JF903785
Typosyllis monilata	Manazuru Peninsula, Japan	EF123860-1	EF123819	EF123781
Typosyllis patriciae	Shark Bay, WA, Australia	JF903665	JF903738	JF903781
Typosyllis pigmentata 1	Manazuru Peninsula, Japan	EF155921		EF123774
T. pigmentata 2	Bamfield, Canada	HM746734	HM746723	FR771740
Typosyllis setoensis	Cassini, Kimberley, WA, Aus	KM277832		

Table 1 (continued)

	Sample site	18S	16S	COI
Typosyllis yallingupensis	Port Denisson, WA, Australia	JF903672	JF903744	
Virchowia clavata	Banyuls-sur-mer, France	AF474314	AF474268	
Xenosyllis scabroides	Lizard Island, QLD, Australia	JF913974	JF903753	
Outgroup				
Nereimyra punctata	GenBank	DQ779661	DQ442577	DQ442566

Typosyllis and *Syllis* species as they were originally described

WA Western Australia, *NSW* New South Wales, *QLD* Queensland, *Aus* Australia

Alignments were performed using the program Mafft version 6 (Katoh et al. 2002) using the iterative refinement method E-INS-i, with default gap open and extension values. The molecular combined alignment is available at www.treebase.org. *Typosyllis* and *Syllis* species are named as they were originally described (Table 1 and the "Results" section) as suggested by Aguado et al. (2012).

The combined molecular data sets (18S, 16S, and COI genes) were analyzed using two optimality criteria: maximum parsimony (MP) and maximum likelihood (ML). MP analyses were performed in TNT (Goloboff et al. 2008) using sectorial searches, ratcheting, drifting, and tree fusing algorithms. All characters were left unweighted and non-additive. Jackknife (JK) support values (Farris et al. 1996) for 1,000 replicates were also generated with TNT. ML analyses of the data sets were conducted with RAxML version 7.0.3 (Stamatakis 2006) using the GTR + G + I model of sequence evolution and a partition scheme letting the parameters be optimized for all three genes separately. Bootstrap support values (B) were estimated from 1,000 pseudoreplicates in RAxML, implementing a rapid bootstrapping algorithm (Stamatakis et al. 2008).

Results

Morphological results

T. antoni n. sp.

Figures 1, 2, 3, 4, 5, 6, 7, and 8

Material examined

Holotype MNCN 16.01/15480, paratypes MNCN 16.01/15468-71, 16.01/15481. Additional material UL. Leipzig aquarium, on algae and sandy bottom.

Comparative material examined

Typosyllis heronislandensis Hartmann-Schröder, 1991. Two paratypes ZMH P-20539.

Description

External anatomy

Holotype with 70 segments and one of the longest complete paratypes with 85 segments, no reproductive signs, 15 mm long, 0.8 mm wide. Before reproduction, specimens can reach up to 80–120 segments. The body is long, cylindrical in section, and ventrally flattened. Dorsal color pattern consists of transversal dark brown lines on dorsum of anterior segments (Fig. 1a–c), one line per segment. Posterior segments have no pigmentation, and digestive tube is visible by transparency (Fig. 1a). The first segment has one curved spot, medially located on the dorsum and strongly pigmented in dark red or brown (Fig. 1a, b). Color pattern is more distinct in the region anterior to proventricle (Fig. 1a). In addition to dark brown transversal lines, proventricle segments occasionally with some dark brown spots on the dorsum that are irregularly distributed. Ethanol-preserved specimens are yellowish and with no pigmentation. Prostomium is wide and long, with two pairs of eyes in trapezoidal arrangement, anterior ones slightly larger than posterior pair, eye spots are absent. Antennae, tentacular, and dorsal cirri are long (Fig. 2a, b, d). Median antenna is inserted on the middle of prostomium, with ca. 30 articles; lateral antennae are shorter, inserted on the anterior margin of prostomium, with ca. 20 articles (Fig. 1a). Palps are triangular, longer than prostomium (Fig. 2c), and fused at base with a distinct median groove. Nuchal organs form two ciliary grooves between prostomium and the first segment. The first segment is similar in length to subsequent segments. Two pairs of tentacular cirri are present; dorsal tentacular cirri are longer than the antennae (Fig. 2a), with ca. 40 articles, ventral ones are shorter than the dorsal ones, with ca. 30 articles. Dorsal cirri are alterning in orientation and length. Long dorsal cirri have ca. 35 articles, and short ones have ca. 20 articles in anterior segments (Fig. 2a); in midbody and posterior segments, long dorsal cirri have ca. 30 articles and short ones ca. 20 articles (Fig. 2e). Longer ones are pointing up and shorter ones pointing down. Spiral glands are inside articles. Ventral cirri digitiform are inserted proximally and reaching tips of parapodia (Fig. 2b, f). Conical parapodia each have

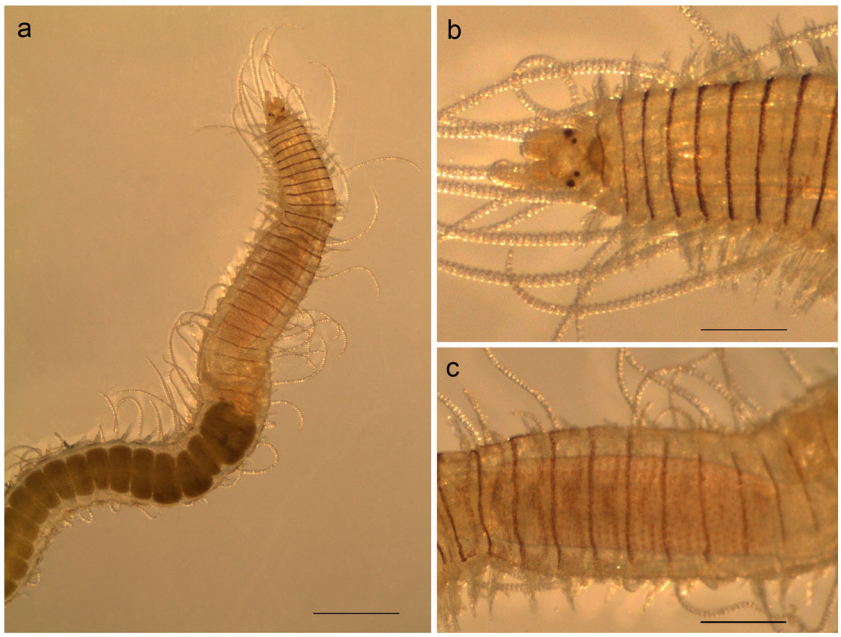

Fig. 1 Light microscopy pictures of *Typosyllis antoni* n. sp. **a** Live specimen, anterior end, dorsal view. **b** Detail of anterior end, dorsal view. **c** Detail of proventricle, dorsal view. *Scales* **a** 0.8 mm; **b**, **c** 0.3 mm

prechaetal and postchaetal lobes, whereas the latter is more distinct (Fig. 2f); lobes are larger in anterior and midbody segments. All chaetae compound and falciger-like, bidentate with distal and proximal teeth similar in length. Spinulation on edge is long, reaching the proximal tooth but not extending beyond it. Anterior parapodia have seven to ten compound chaetae, bidentate blades, gradating in length (most dorsal ca. 28 μm, most ventral ca. 14 μm), and blade edge has long spines through the whole edge (Figs. 3a–c and 4a–c); most distal spines reach the level of the proximal tooth (Fig. 4b). Midbody parapodia have six to seven compound chaetae, blades bidentate, similar in length to anterior ones, with long spines through the whole edge (Fig. 3d–f); most distal spines reach the level of the proximal tooth (Fig. 4e, f). Posterior chaetigers have four to six compound chaetae, blades bidentate, shorter than those of anterior chaetigers (most dorsal ca. 24 μm, most ventral ca. 10 μm) and have long spines through the whole edge (Fig. 3g, j); most distal spines reach the level of the proximal tooth (Fig. 4j–m). Most ventral chaetae are in posterior segments with pointed shafts (Figs. 4l and m). Posterior segments have one bidentate ventral simple chaeta (Figs. 3h and 4h) and one dorsal simple chaeta with a distal notch (Figs. 3h, i and 4g). Ventral and dorsal simple chaetae have small spines on distal end (Figs. 3h, i and 4h). Anterior parapodia have three to four pointed aciculae, one to two slightly distally bent (Fig. 4d); midbody parapodia have two to three pointed aciculae and one thin acicula in addition. Occasionally, one to two aciculae are protruding from parapodia. Most posterior segments have one pointed acicula and one additional thin acicula (Fig. 4i). Pygidium conical, with two anal or pygidial cirri (ca. 30 articles) and one median papilla (Fig. 3l) present in most of the specimens. Articles of anal cirri have pores (Fig. 3k).

Internal anatomy

The musculature of the body wall is characterized by two major muscle systems, the outer transversal arranged muscle fibers (often named circular muscle fibers in other annelids) and the inner longitudinal muscles (Figs. 5b–d and 6a). Whereas the longitudinal muscle fibers form distinct bundles, the transverse fibers form a dense meshwork of fibers partly encircling most parts of the dorsal and ventral body (Fig. 5b, c). Notably, the transverse fibers do not form a prominent layer embracing the whole animal but exhibit a gap of fibers at the ventral side and therefore cannot be named circular (Fig. 6b). Furthermore, most dorsal fibers being part of the outer muscle layer are not restricted to only one parapodial region. These fibers interconnect two parapodial regions and as a consequence, represent a diagonal cross bracing pattern. The latter pattern is most prominent in anterior dorsal regions (Fig. 5c) but is lacking in posterior body parts.

Whereas the transverse fibers form a consistent outer layer, the longitudinal fibers are arranged in prominent bundles. Thus, two prominent longitudinal muscle bundles are situated each at the dorsal and ventral side (Figs. 5b–d and 6a–c). Notably, the dorsal longitudinal bundles are represented by two distinct muscular plates (Fig. 6a). The anterior origin of the dorsal bundles can be found in the antennal region, whereas the ventral bundles originate anteriorly to the first chaetiger (Fig. 5b). The pygidium lacks distinct longitudinal and transverse muscle bundles (Fig. 5d).

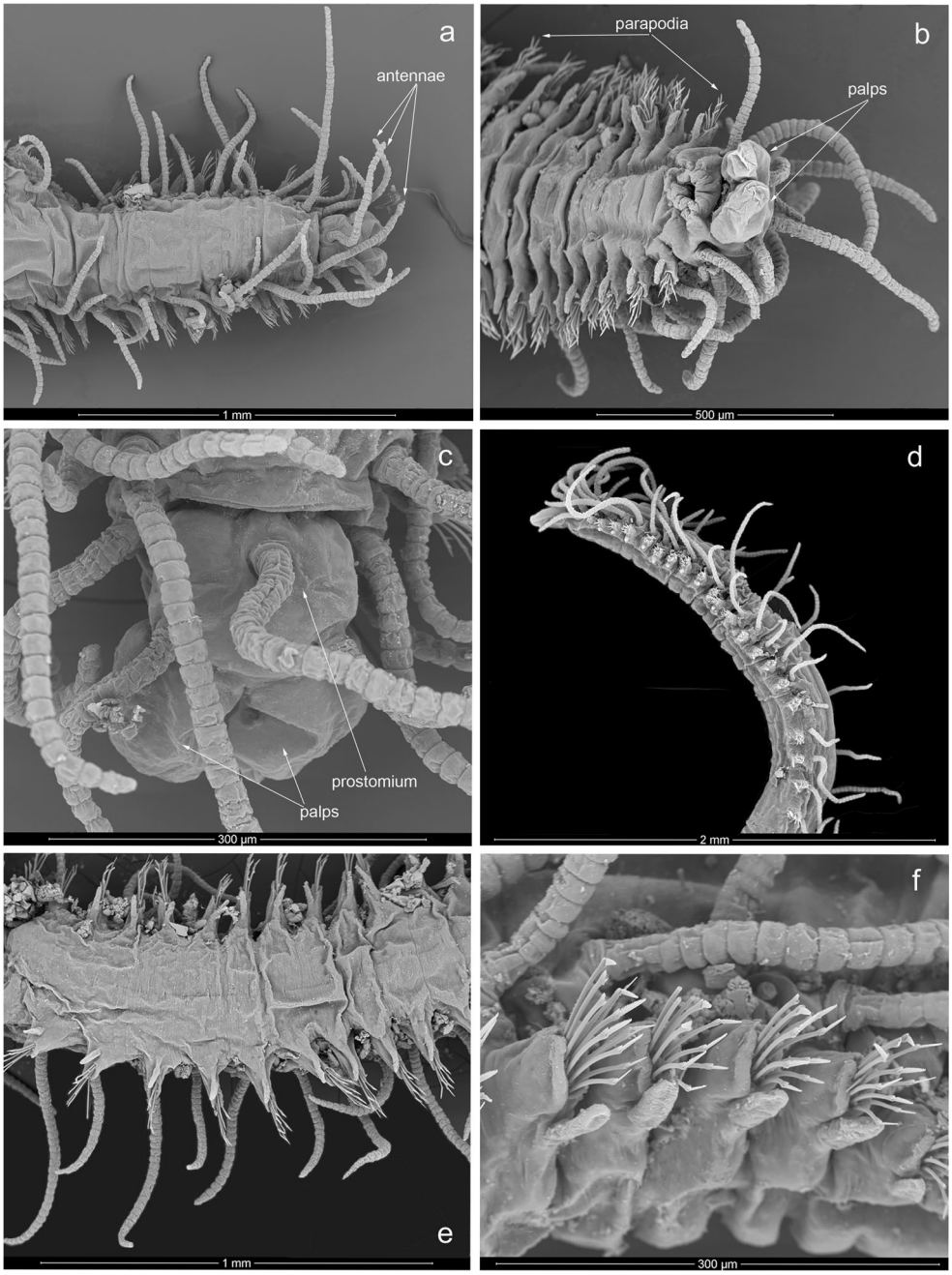

Fig. 2 SEM images of *Typosyllis antoni* n. sp. **a** Anterior end, dorsal view. **b** Anterior end, ventral view. **c** Detail of anterior end, dorsal view. **d** Anterior end, lateral view. **e** Midbody segments, ventral view. **f** Midbody parapodia, lateral view

Palp muscles insert in dorsal anterior regions, anterior of the antennal base (Fig. 5a, b). The musculature is represented by a prominent median muscle fiber and weaker muscle fibers branching off the main muscle. Notably, the margin of the palps lacks muscle fibers. The antennae and dorsal and ventral cirri are quite similar in terms of muscle arrangement (see Fig. 5a–f). Each antenna and cirrus is formed by inner longitudinal muscle fibers running from the base to the apex (Fig. 5a–c, e). In the dorsal cirri, additional lateral F-actin staining is visible, exhibiting a striped pattern (Fig. 5f). The base of the dorsal cirri is formed by distinct cirral muscle bundles (Fig. 6a) possessing a basal muscular socket. The base of the antennae is represented by a muscular socket, too (Fig. 5a). In contrast to the dorsal cirri, the antennal base is formed by separate muscle fibers terminating in the region of the peristomium (Fig. 6a).

The uniramous parapodia insert laterally between the dorsal and ventral longitudinal muscle bundles (Fig. 6a). The parapodium itself consists of distinct parapodial retractor muscles forming the parapodial cone and prominent acicular protractor muscles inserting at the aciculae (Fig. 6a). The latter muscle fibers terminate at the aciculae and under the epidermis, in close proximity to the longitudinal muscle bundles. Furthermore, the acicular flexor muscle terminates at the acicular base and runs towards ventral where it is anchored

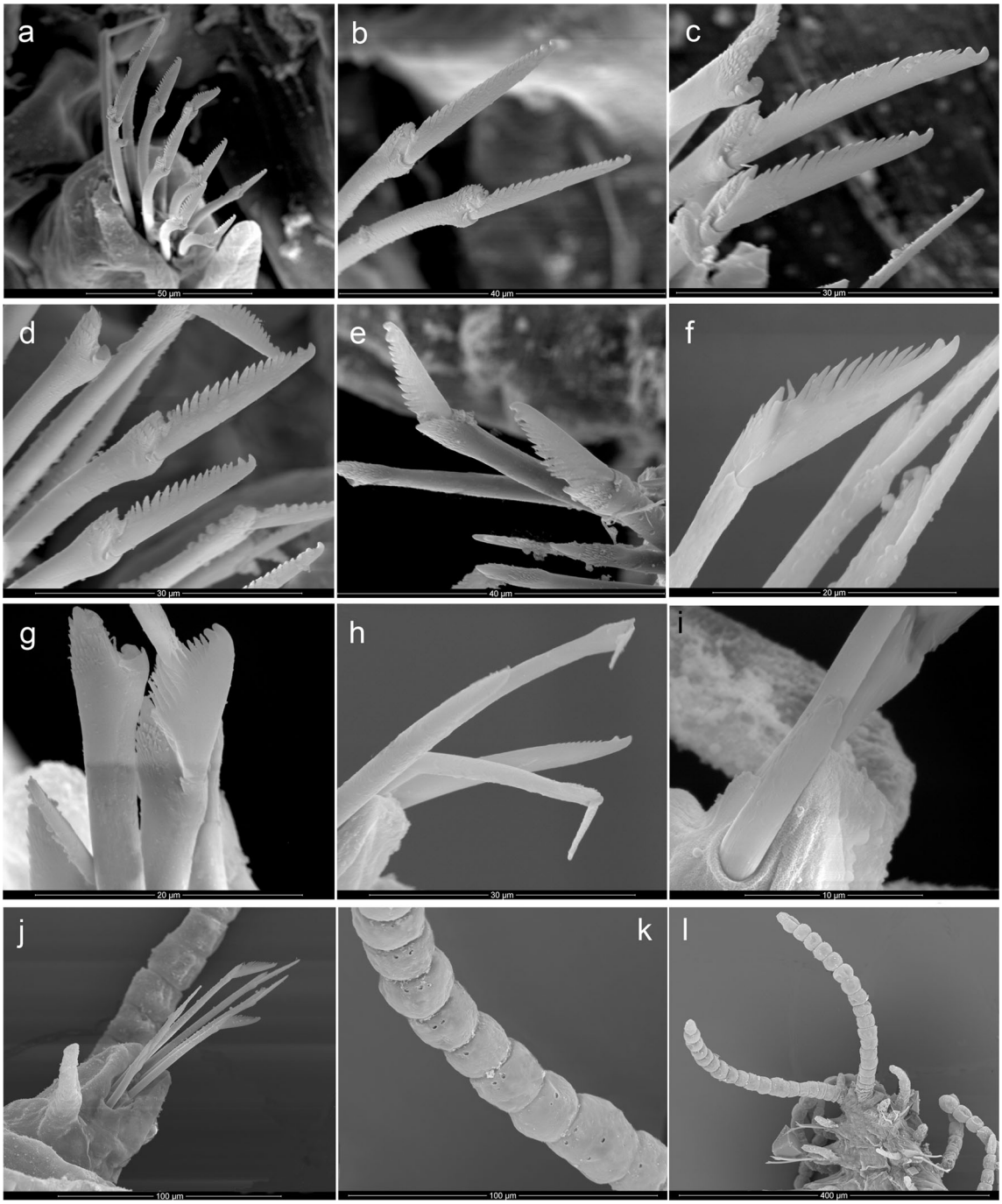

Fig. 3 SEM images of *Typosyllis antoni* n. sp. **a** Chaetae fascicle, anterior parapodium. **b**, **c** Most dorsal chaetae, anterior parapodium. **d**, **e** Most dorsal chaetae, posterior parapodium. **f** Medially located chaetae, posterior parapodium. **g** Most ventral chaetae, posterior parapodium. **h** Dorsal and ventral simple chaetae, posterior parapodium. **i** Dorsal simple chaeta, posterior parapodium. **j** Chaetal fascicle, posterior parapodium. **k** Anal cirri, detail of pores. **l** Pygidium and anal cirri, ventral view

between the ventral longitudinal muscle fibers (Fig. 6a). Another distinct muscle bundle is formed by the chaetal flexor muscle that runs from the apical chaetae toward ventral and terminates in the region of the median muscle bundle (Fig. 6a). Additionally, the base of the dorsal cirrus is formed by cirral muscle fibers that run from the parapodial cone toward the cirral base (Fig. 6a).

The internal pharynx is similar in length to the prominent proventricle. Thus, the whole structure is visible through 13–15 segments, and the proventricle itself extends through eight segments (Fig. 1c), with about ca. 30 rows of muscular cells, visible by transparency and cLSM (Fig. 6d, e). Furthermore, a tooth on the anterior margin (Fig. 1a, b) and ten distal papillae are visible (Fig. 5a, b). The pharynx musculature is

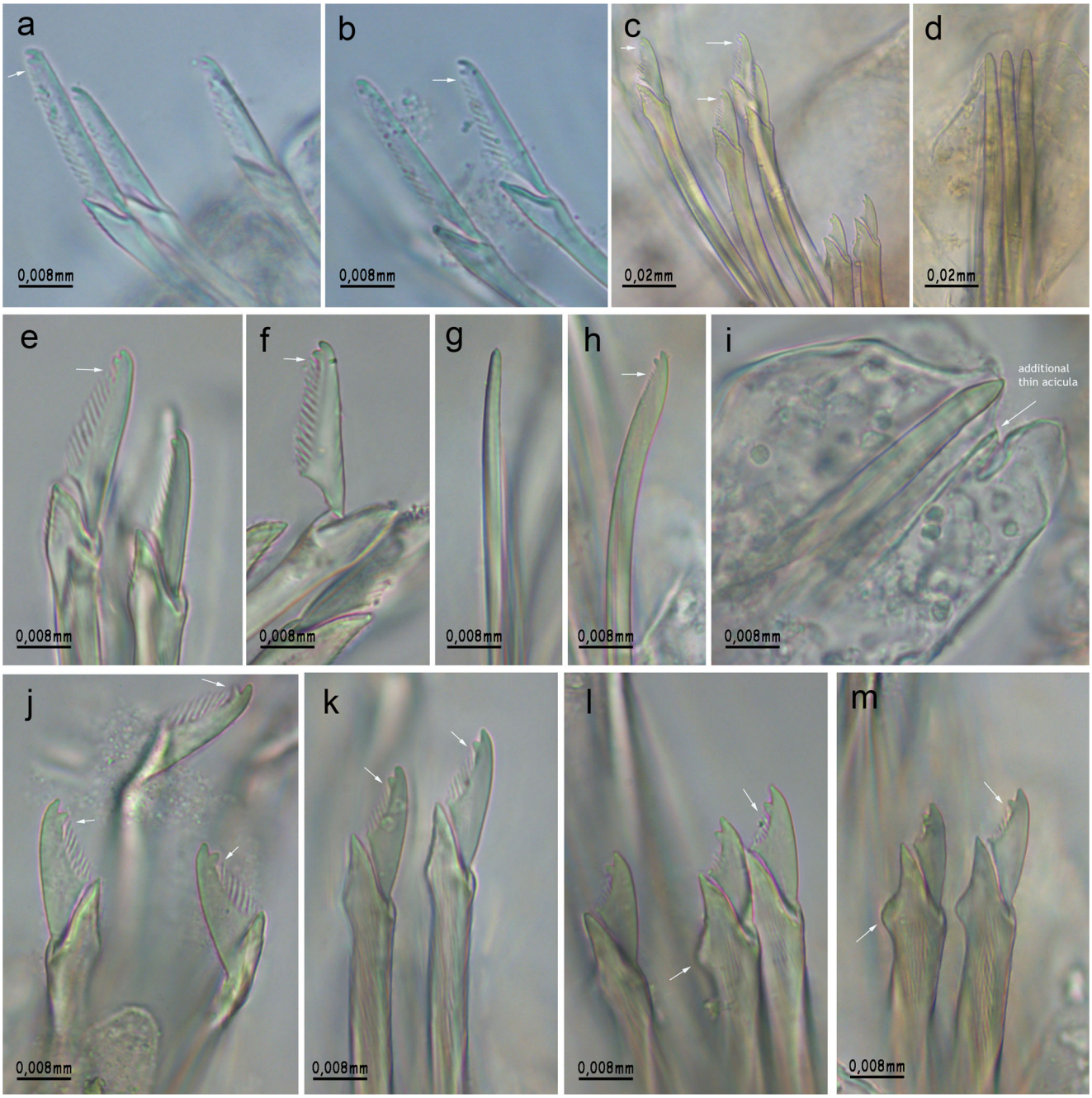

Fig. 4 Light microscopy pictures of *Typosyllis antoni* n. sp. **a** Anterior chaetae, most dorsal ones and medially located in the fascicle. **b** Anterior chaetae, most dorsal ones. **c** Anterior chaetae, medially and most ventral ones. **d**. Anterior aciculae. **e** Midbody chaetae, most dorsal ones and medially located in the fascicle. **f** Midbody chaeta, most dorsal one. **g** Dorsal simple chaeta, posterior parapodium. **h** Ventral simple chaeta, posterior parapodium. **i** Posterior aciculae. **j** Posterior chaetae, most dorsal ones and medially located in the fascicle. **k** Posterior chaetae, most dorsal ones. **l**, **m** Posterior chaetae, most ventral ones. *Arrows* pointing the distal spines that reach the level of the proximal tooth and pointed posterior shafts (**l**, **m**)

represented by a dense meshwork of longitudinal and circular muscle fibers, which form a tube (Fig. 5a). The proventricle almost fills out the entire body cavity (Fig. 6b) of the anterior animal. Forming a muscular tube, the proventricle has a slit-like passage where the intestine is located (Fig. 6b). The staining against serotonin reveals a strong homogenous serotonergic immunoreactivity within the whole proventricle (Fig. 6c). The muscular tube itself is formed by honeycomb-like radial muscle bundles in ca. 30 rows, which are enveloped by distinct circular muscle fibers (Fig. 6d). At the anterior end of the proventricle, prominent suspending muscles are exhibited, anchoring the proventricle within the body cavity. Furthermore, the anterior end of the proventricle is characterized by a tube-like anterior circular muscle layer (Fig. 6d).

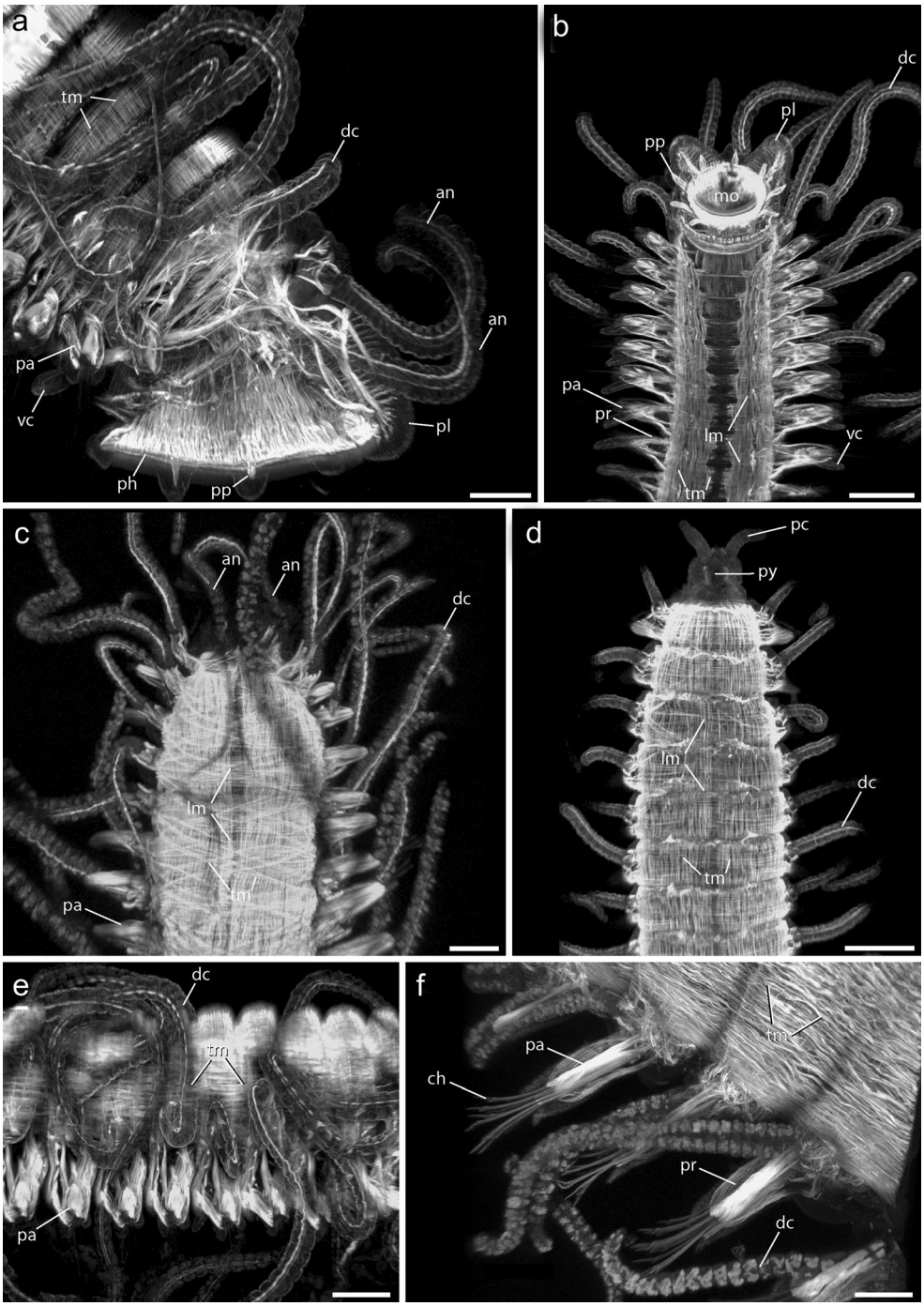

Fig. 5 Confocal maximum projections of *Typosyllis antoni* n. sp. Phalloidin–rhodamine labeling of adult specimens. Anterior is up in **b** and **c**, down in **a** and **d**, and right in **e** and **f. a** Lateral view of the anterior region, with everted pharynx (*ph*) and prominent dorsal cirri (*dc*), antennae (*an*), and palps (*pl*). The antennae exhibit prominent basal muscular sockets (*dotted ring*). **b** Ventral view of the anterior region showing the distinct longitudinal muscle bundles (*lm*) and the transverse muscle fibers (*tm*) forming semicircular fibers. **c** Dorsal view of the anterior region. Distinct longitudinal muscle fibers (*lm*) and the partly diagonal cross bracing transverse muscle fibers (*tm*) are exhibited. **d** Dorsal view of the posterior end showing the prominent pygidium (*py*) lacking distinct muscle bundles and the pygidial cirri (*pc*). **e** Lateral view of the midbody region, dorsal is up. The dorsal cirri (*dc*) insert at the base of the parapodium (*pa*). **f** Dorsolateral view of a midbody parapodial region. The dorsal cirri (*dc*) are represented by a prominent staining exhibiting a striped pattern; *an* antenna, *ch* chaetae, *dc* dorsal cirrus, *lm* longitudinal muscle fiber, *mo* mouth opening, *pa* parapodium, *pc* pygidial cirri, *ph* pharynx, *pl* palps, *pp* pharyngeal papillae, *pr* parapodial retractor muscle, *py* pygidium, *tm* transverse muscle fiber, *vc* ventral cirrus. *Scale bar*= 100 μm

After the proventricle, there is the ventricle, followed by two caeca. Methylene blue staining reveals spherical structures within the caeca strongly pigmented in blue.

Reproduction

Long specimens (usually with 80–120 segments) develop stolons. Stolonization seems to occur once a month under laboratory conditions (when temperature is more than 24 °C, circadian rhythm with 12 h light). Adults produce gametes in their midbody and posterior segments (approximately from segments after the proventricle until the pygidium). Small disturbances provoke the animal to release gametes laterally, possibly through the nephridia (Fig. 7g). When the stolon is formed and still attached to the parental body, gametes move toward the posterior segments (Fig. 7d, f). Stolons are dicerous, with two anterior lobes, two pairs of conspicuous eyes and two small antennae anteriorly located (Fig. 7e). Female stolons are

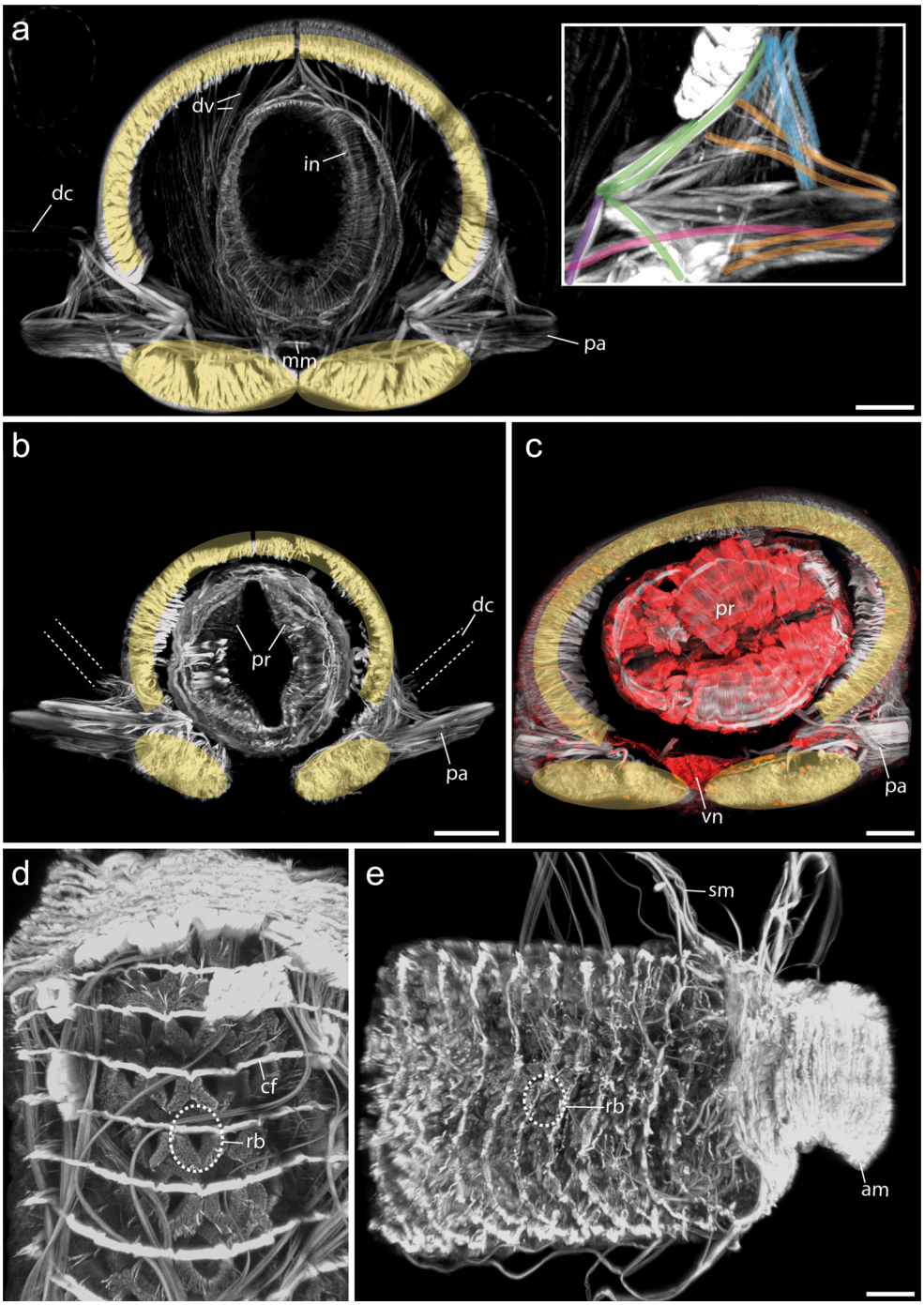

Fig. 6 Confocal maximum projections of *Typosyllis antoni* n. sp. Phalloidin–rhodamine (*gray*) and serotonin labeling (*red*) of cross sections (**a**–**c**) and the proventricle (**d**, **e**) of adult specimens. Dorsal is up in **a**–**c**. Anterior is up in **d** and right in **e. a** Cross section of the midbody region, the prominent longitudinal muscle bundles are colored in *yellow*. The *insert* shows a detailed view of the parapodium, and major muscle bundles are color coded—parapodial retractor muscle in *brown*, acicular protractor muscle in *green*, acicular flexor muscle in *violet*, chaetal flexor muscle in *pink*, cirral muscle bundle in *blue*. **b** Cross section showing the distinct proventricle (*pr*) filling almost the whole body cavity. The longitudinal muscle bundles are color coded in *yellow*. **c** The proventricle (*pr*) and the ventral nerve cord (*vn*) show distinct serotonergic immunoreactivity. **d** The separated proventricle (*pr*) exhibits radial honeycomb-like muscle bundles (*rb*, *dotted circle*) and prominent circular muscle fibers (*cf*) surrounding the whole structure. **e** The separated proventricle (*pr*) is represented by an anterior circular muscle bundle (*am*) and suspending muscles (*sm*) terminating at the border between the anterior circular muscle bundle (*am*) and the radial muscle bundles (*rb*). *am* anterior circular muscle bundle, *cf* circular muscle fiber, *dc* dorsal cirrus, *dv* dorsoventral muscle fibers, *in* intestine, *mm* median muscle bundle, *pa* parapodium, *pr* proventricle, *rb* radial muscle bundle, *sm* suspending muscle fiber, *vn* ventral nerve cord. *Scale bar*=100 μm (color figure online)

full of spherical oocytes gray in color (Fig. 7b, d) and male stolons with two yellowish packages of sperm per segment (Fig. 7a, c). *Typosyllis antoni* n. sp. shows sequential hermaphroditism.

Ecology

Animals live at the bottom, often within the soft sediments. They feed on algae. All the specimens have been found with some algae material in their digestive tubes.

Regeneration

T. antoni n. sp. regenerates anteriorly and posteriorly. After dissection, the wound site constricts by musculature, forming an invagination of the first remaining segment. Two days after dissection, blastema formation occurs in anterior regenerating specimens, whereas this process is delayed in posterior regeneration. Both anterior and posterior regenerating specimens bear a well-developed blastema after 3 days. Four days after dissection, the regenerated anterior end bears a prostomium

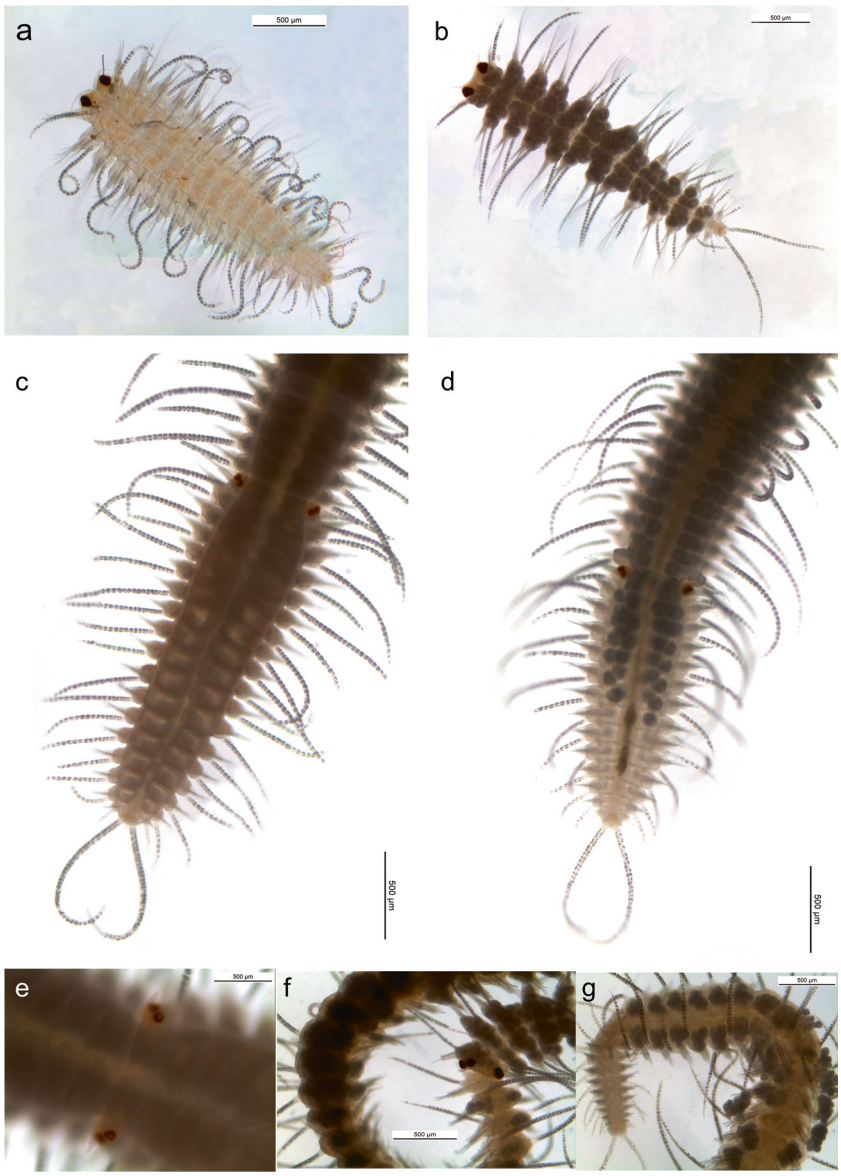

Fig. 7 *Typosyllis antoni* n. sp. **a** Male stolon, dorsal view. **b** Female stolon, dorsal view. **c** Male stolon still attached to the parental body, dorsal view. **d** Female stolon still attached to the parental body, dorsal view. **e** Detail of anterior appendages of male stolon, dicerous kind, dorsal view. **f** Ovaries within posterior segments of parental body and female stolon still attached. **g** Posterior segments with ovaries of a female that has not developed a stolon yet

with developing antenna, palps, and eyes (Fig. 8a). Additionally, new segments become visible, with regenerating tentacular cirri in the first segment. The number of re-established anterior segments varies between two and three in different specimens but is limited to the initially existing number. At the same stage, the posteriorly regenerating specimens exhibit a pygidium with developing anal cirri and a median papilla (Fig. 8b). During the following days, the anterior structures grow and 6 days after dissection, a pharynx is visible (Fig. 8c), connecting the intestine with the mouth opening. In posterior regenerating specimens, the process is continued by addition of segments, first visible at day 5. After 6 days, posterior segments bear cirri and chaetae become visible (Fig. 8d). Moreover, the anal cirri have developed the first articles. The second week is dominated by growth in both cases of regeneration. Regenerated anterior and posterior ends are still small, but the difference to the residual body segments becomes indistinct. Remarkably, there are no signs of a regenerated proventricle, ventricle, caeca, or pharyngeal tooth in the anterior part (Fig. 8e). In contrast, the posterior regenerating specimens reach the original adult shape (Fig. 8f). Many of the anterior regenerating specimens develop gametes and stolons. In both plastic bowls as well as in the control, specimens with regenerating posterior ends and complete untouched ones show signs of stolonization. Free stolons were also observed during the experiment. Further experiments show evidence of regeneration in more than two anterior chaetigers when individuals are dissected directly in front of the proventricle. Moreover, when dissecting between chaetigers 35 and 36 or when dissecting directly behind the proventricle, decapitated specimens produced two or three sequential stolons in a few

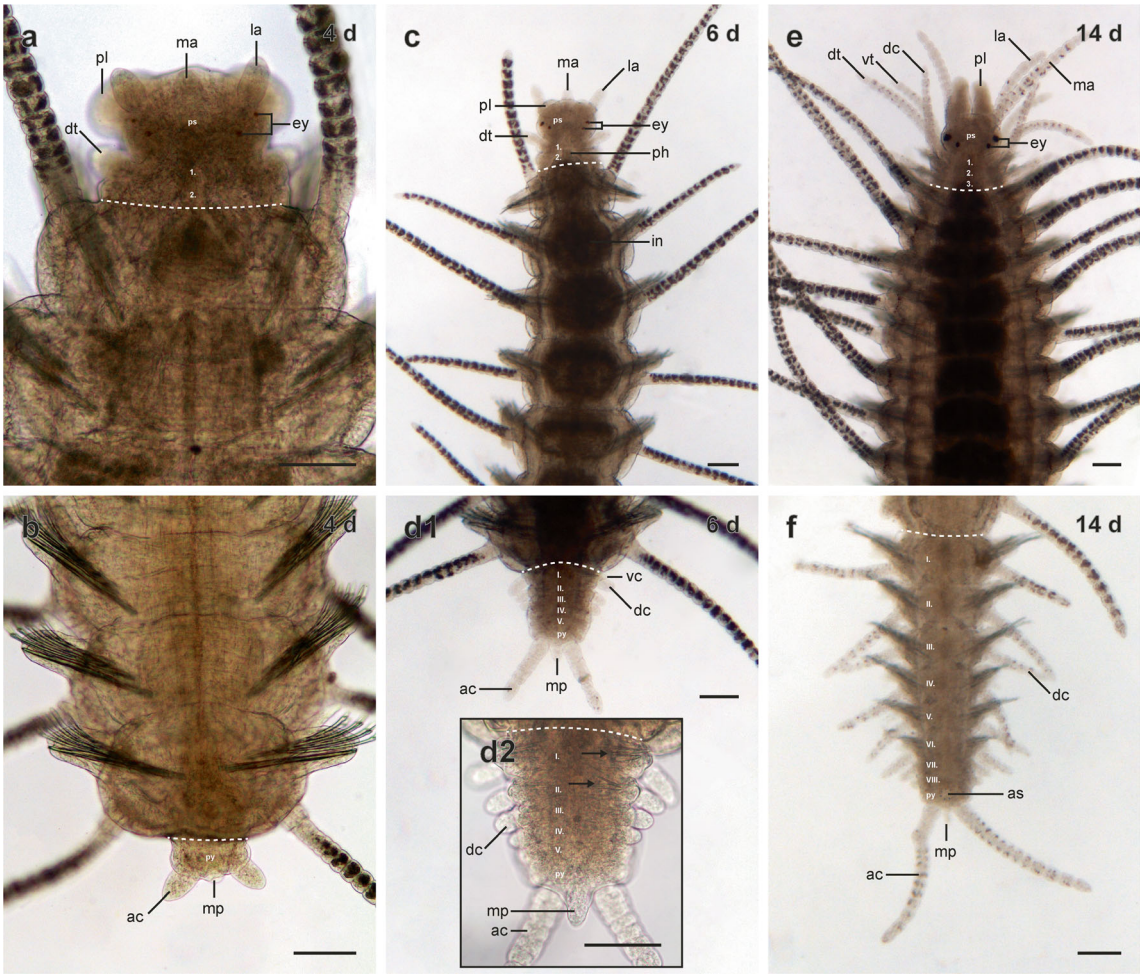

Fig. 8 Light microscopy pictures of regenerating specimens of *Typosyllis antoni* n. sp. All pictures are dorsal views except **d2** (ventral view). **a**, **c**, **e** anterior end, **b**, **d1**, **d2**, **f** posterior end. The *dotted white line* indicates the site of dissection. **a** At 4 days after dissection, the re-developing prostomium (*ps*), as well as the first two segments (*1*, *2*) are visible (in other specimens also three segments were observed). The prostomium shows palps (*pl*), antenna (*la*, *ma*) and two pairs of eyes (*ey*). Dorsal tentacular cirri (*dt*) of the first segment occur. **b** After 4 days, the pygidium (*py*) with the anal cirri (*ac*) and the median papillae (*mp*) are regenerated. **c** At 6 days, all in **a** described anterior structures have grown. Pharynx (*ph*) is re-developed, connecting the mouth opening (not visible) with the intestine (*in*). **d1**, **d2** The posterior end is well regenerated after 6 days, with five segments (*I–V*). The older segments have re-developed their cirri (*dc*, *vc*) and the chaetae (*arrows*). **e** The regeneration of the anterior end is at an advanced stage after 14 days. Any signs of proventricle, ventricle, or ceca or pharyngeal tooth are missing. **f** At 14 days, the regeneration of the posterior end has nearly finished. *1–3*, regenerated anterior segments; *I–VIII*, regenerated posterior segments; *ac* anal cirrus, *as* anus, *dc* dorsal cirrus, *dt* dorsal tentacular cirrus, *ey* eye, *in* intestine, *la* lateral antenna, *ma* median antenna, *mp* median papilla, *ph* pharynx, *pl* palp, *ps* prostomium, *py* pygidium, *vc* ventral cirrus, *vt* ventral tentacular cirrus. *Scale bar*=100 μm

cases. In one case, the regeneration of the posterior end occurred, while the stolon was still attached. Finally, regeneration of posterior segments after stolonization appears to be delayed, when specimens where dissected between chaetigers 35 and 36.

Remarks

Considering external morphological features, *T. antoni* n. sp. is different to all other species of the *Syllis-Typosyllis* group in the following combination of characters: color pattern consisting in transversal red lines on the dorsum of anterior segments; antennae and dorsal cirri long, the latter with strong alternation in length; bidentate chaetae falciger-like with proximal and distal teeth similar in length and long spinulation on edge; one tiny and thin acicula appearing in posterior segments in addition to thicker and pointed one and a long proventricle.

T. antoni n. sp. is most closely related to *T. heronislandensis* Hartmann-Schröder 1991 (from East Australia). It is similar to this species and *Syllis parturiens* Haswell 1920 (Gulf of Aqaba and Australia) (not included herein) in chaetae shape (Hartmann-Schröder 1991; Haswell 1920). However, *T. heronislandensis* and *Typosyllis parturiens* have different spinulation; long spines are restricted to the base of anterior blades, while they become much

shorter through the distal end (Hartmann-Schröder 1991; Licher 1999). In *T. antoni* n. sp., the spinulation is long through the whole edge in all the chaetiger blades from anterior and posterior segments. In all blades, most distal spines remain long and reach the level of proximal tooth (see arrows in Fig. 4). Additionally, *T. heronislandensis* has short dorsal cirri, and *S. parturiens* is viviparous (Licher 1999). Moreover, *T. heronislandensis* seem to lack a distinctive color pattern (Hartmann-Schröder 1991), although this is usually not a good diagnostic character since specimens frequently loose coloration when they are preserved. Finally, none of these two species have an additional thin acicula in the posterior segments. *Typosyllis horrockensis* Hartmann-Schröder 1981 (from West Australia) is a similar species in the shape of blades and color pattern of live specimens, but it has short dorsal cirri and short spinulation of blades (Hartmann-Schröder 1981; Licher 1999). *Typosyllis filidentata* Hartmann-Schröder 1981 (Patagonia and West Australia) has chaetae with long spinulation (Hartmann-Schröder 1979); however, shape of blades and length and orientation of spines is different to those found in *T. antoni* n. sp. *T. antoni* n. sp. is also characterized, among other features, by the curvature of the distal and proximal teeth of blades. Similar shape of blades' teeth is found in *Syllis augeneri* Haswell 1920 (Australia and Indonesia) and *Typosyllis edensis* Hartmann-Schröder, 1989 (Australia) (Hartmann-Schröder 1989; Haswell 1920; Licher 1999; Aguado et al. 2008). However, these species have shorter dorsal cirri and different aciculae.

As stated above, another distinct feature of *T. antoni* n. sp. is the presence of an additional considerably thin acicula in posterior segments. This kind of acicula has been described before for other species, such as *Syllis westheidei* (San Martín 1984) (from Galapagos, Red Sea, and Mediterranean Sea) and *Typosyllis magna* (Westheide 1974) (from Galapagos, and Gulf of Aqaba). However, none of these species share all the characteristics of *T. antoni* n. sp. *S. westheidei* has a different shape of blades and color pattern, and *Syllis magna* has pseudospiniger or spiniger-like blades.

Etymology

This species is dedicated to Anton Helm, who was born approximately when the first specimens were studied and identified as possibly new.

Phylogenetic results

The results of the different methodologies when analyzing the combined data set widely agree in the recovered topologies, excepting for the position of some few taxa (Figs. 9 and 10). The main differences regard to the placement of *Parahaplosyllis brevicirra* Hartmann-Schröder 1991, which is sister to *Syllis alternata* Moore, 1908, in ML results (Fig. 9), while sister to *Trypanosyllis*/*Xenosyllis*/*Eurysyllis* clade in MP (1 most parsimonious tree (MPT), 15,354 steps) (Fig. 10); in both cases, support values are not high (B, 72 %; JK, 56 %). Another difference when comparing both topologies (Figs. 9 and 10) is the position of clade 2, but again, support values of its sister relationships are, in both cases, considerably low.

Results show the monophyly of Syllinae well supported, mainly in the ML result (B, 94) (Fig. 9). The sister group of Syllinae is the monophyletic genus *Perkinsyllis* Aguado and San Martín 2009. Syllinae is divided into different clades, some of them with high support values, such as the following: *Trypanosyllis*/*Xenosyllis*/*Eurysyllis*; *Haplosyllis* Langerhans, 1879; *Branchiosyllis* Ehlers, 1887; *Paraopisthosyllis* Hartmann-Schröder, 1991; *Megasyllis* San Martín, Hutchings, and Aguado, 2008; clade 1 and clade 2. The genera *Typosyllis*, *Syllis*, and *Opisthosyllis* are not monophyletic (Figs. 9 and 10).

A sister group relationship of *T. antoni* n. sp. and *T. heronislandensis* Hartmann-Schröder, 1991, is supported by both methodologies (ML and MP) and by very high support values (B and JK, 100) (Figs. 9 and 10). *Syllis*/*Typosyllis* species with spiniger-like chaetae are located within clade 1 (such as *Typosyllis yallingupensis* Heacox and Schroeder, 1982, and *Syllis garciai* Campoy, 1982). *Syllis*/*Typosyllis* species with simple chaetae that appear after a fusion process of shafts and blades (such as *Syllis gracilis* Grube, 1840; *Syllis ypsiloides* Aguado, San Martín, and Ten Hove, 2008, and *S.* cf. *gracilis australiensis* Hartmann-Schröder, 1979) are located in different clades.

Discussion

T. antoni n. sp. as a model for evolutionary studies in Syllinae

The number of new species within Syllidae is increasing considerably (San Martín and Aguado, accepted), especially during the last decades. Increasing number of detailed descriptions and comprehensive studies about Syllidae (Aguado et al. 2007, 2012; Aguado and San Martín 2009) enable now the localization and description of new taxa within this group. We provide herein a description of a new species, *T. antoni* n. sp., which includes information obtained from several different techniques (light microscopy, SEM, cLSM, and molecular phylogenetic analyses). This study may constitute a framework for future descriptions of Syllidae. The phylogenetic analyses performed herein include most of all available data for species of Syllinae (a total of 86 from the GenBank, plus 4 more from Australia included for the first time for this study). We find that *T. antoni* n. sp. is closely related to *T. heronislandensis* from Australia (see the "Remarks" section). This sister group

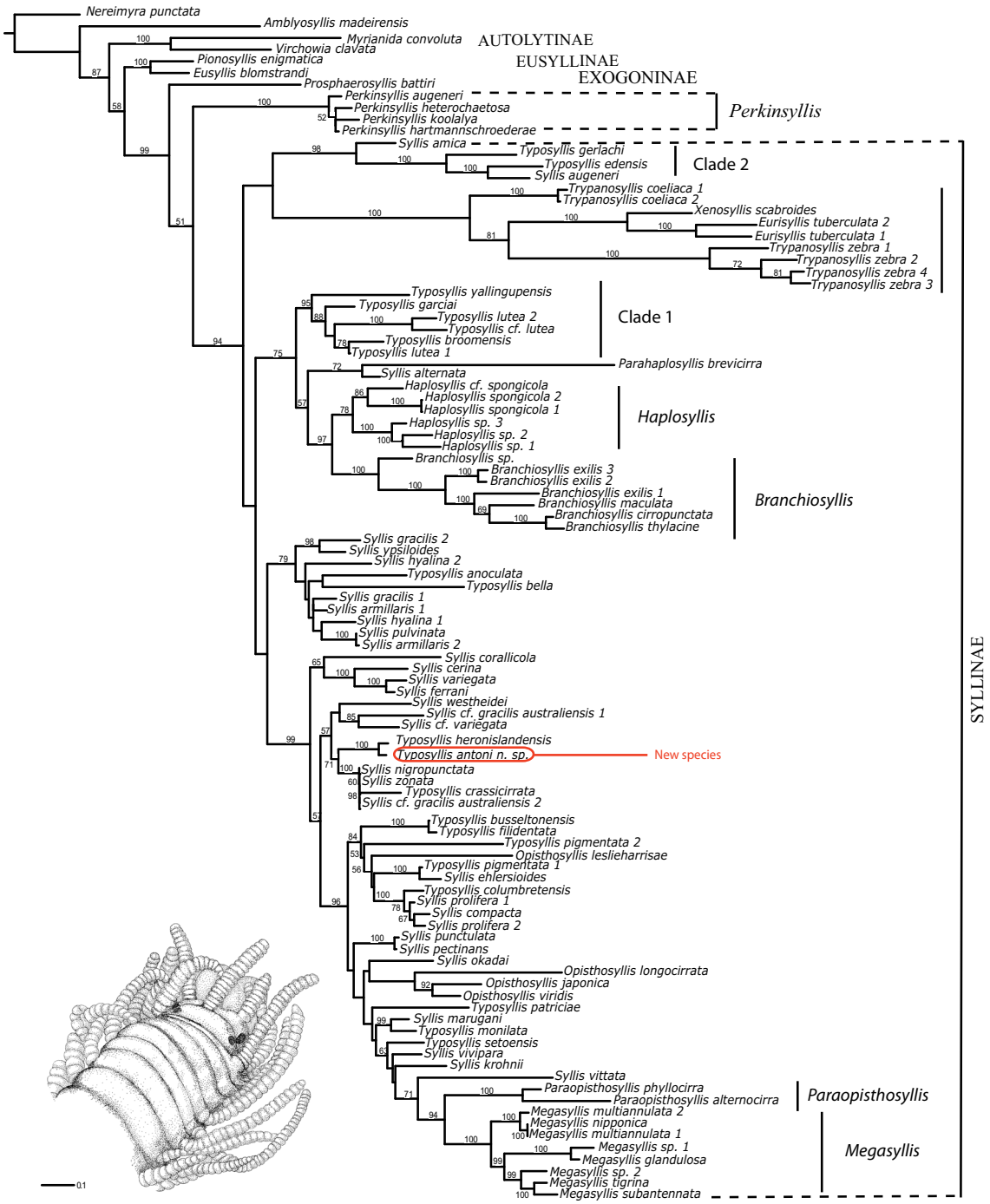

Fig. 9 Maximum likelihood tree. Bootstrap support values above nodes. *Syllis* and *Typosyllis* species as they were described. *Drawing*: *S. marugani* (after Aguado et al. 2006)

relationship supports the generic assignation of the new species proposed herein as *Typosyllis*. Moreover, our results indicate a pacific origin for the species, which was introduced into our seawater aquarium. A potential source could be so called living stones purchased from an aquarium shop which originate from Indonesia.

Whereas the natural source location for this newly described species remains unclear, the available data makes it immediately to one of the best investigated syllids, emphasizing its potential as model for the whole group. *T. antoni* n. sp. can be kept in artificial seawater over long times (at least more than 2 years in the Leipzig facility, yet), where it also reproduces sexually. This could be documented through male and female stolons, which can be observed regularly (under the here described conditions, a monthly cycle is assumed). Additionally to sexual reproduction, we were able to

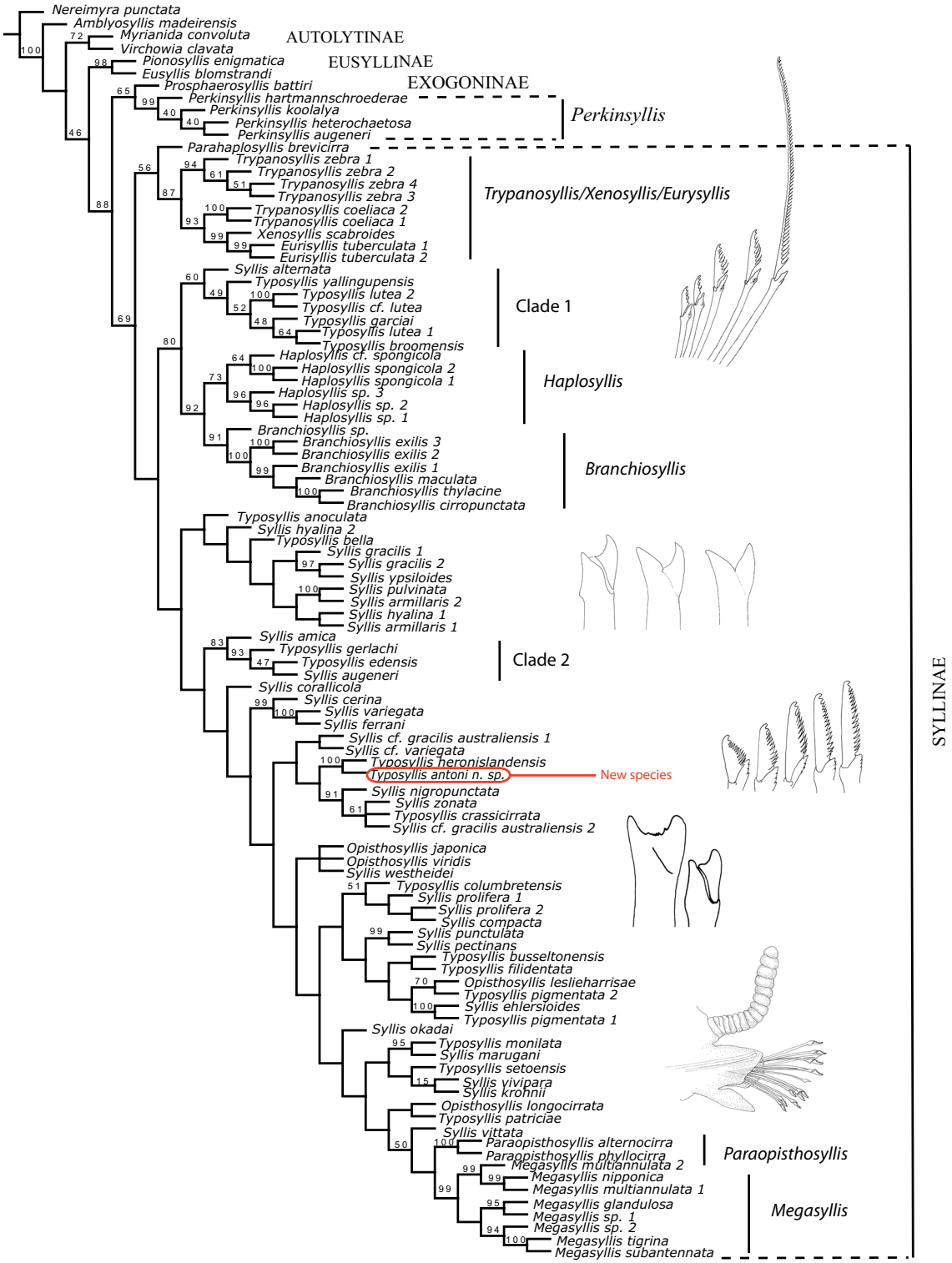

Fig. 10 Most parsimonius tree. Jacknife support values above nodes. *Syllis* and *Typosyllis* species as they were described. *Drawings from up to down*: chaetae of *Syllis benbeliahue* (after Aguado and San Martín 2006), *Syllis ypsiloides* (after Aguado et al. 2008), *Typosyllis antoni* n. sp., *Syllis gracilis australiensis*, and parapodium of *S. marugani* (after Aguado et al. 2006)

demonstrate the regeneration ability of this species. We find that the anterior as well as the posterior end regenerate, even though until now, we find no evidence for the regeneration of the proventricle. Moreover, available Illumina-based transcriptomic data for *T. antoni* n. sp. (Weigert et al. 2014, see accession SRX513556 in the NCBI short read archive)

enables future gene expression studies in this and closely related species, as primer for conserved regions of genes of interest might be designed for many other Syllinae. Besides available molecular data, we provide a detailed description of the musculature by F-actin staining coupled with cLSM. Our experiments show that these animals are well suited for microscopic studies due to their size and transparency. Besides this, standard immunocytochemical protocols work well for *T. antoni* n. sp. In summary, we suggest that this species is well suited for evolutionary studies connected to reproduction and regeneration. Phylogenetically related species of the *Syllis-Typosyllis* complex may show similar characteristics and should be also considered for this type of studies.

The morphology of ***T. antoni*** n. sp

Considering internal anatomy, a comparison can be made with *Myrianida prolifera*, the only syllid species whose musculature system has been previously studied via cLSM investigations so far (Filippova et al. 2010). With a presence of four longitudinal muscle bundles, a body wall containing transverse fibers in a supralongitudinal and diagonal cross bracing position, a proventricle with honeycomb-like radial muscle fibers arranged in distinct rows, and prominent dorsal and ventral cirri with longitudinal myofilaments, both species share a similar pattern of body wall musculature. Such an arrangement of longitudinal muscle bundles and transverse (or often named circular) muscle bundles can be found in other members of the Errantia as well (see Tzetlin and Filippova 2005; Purschke and Müller 2006). Prominent transverse muscle fibers are described also for Hesionidae, Nereididae, Phyllodocidae, and Myzostomida (Storch 1968; Tzetlin and Filippova 2005; Helm et al. 2013). Additionally, a similar arrangement and presence of parapodial muscle fibers can be seen in groups like, e.g., the Aphroditidae, Polynoidae, Nereididae, Sphaerodoridae, and Myzostomida (Storch 1968; Tzetlin and Filippova 2005; Filippova et al. 2010; Helm et al. 2013). Our data shows that the muscular patterns of errant Annelida show many similarities which may trace back to their last common ancestor.

The proventricle of Syllidae is a complex structure that seems to be unique in the Metazoa (del Castillo et al. 1972). However, the function of this structure remains dubious, even though it is speculated to be related to the unique reproductive modes in Syllidae among annelids (Aguado and San Martín 2009). Apart from a digestive function, it might also carry an endocrine function. Some experiments suggest that it plays an important role in the regulation of the hormonal activity, especially during the reproductive cycle by segregating the hormones that inhibit new stolonizations while stimulating the regeneration of the posterior part of the body (Franke 1983, 1986; Heacox and Schroeder 1982). When the levels of these hormones decrease the stolonization starts. Interestingly, connected to the posterior part of the proventricle, we find a pair of caeca, which were described as T-shaped glands by other authors (Jeuniaux 1969). A glandular function of these sacs is further indicated by our methylene blue staining. In contrast, the proventricle is mainly characterized by a strong musculature, as well as strong serotonergic signal throughout the structure. We speculate that the putative endocrine activity of the proventricle may in fact be the activity of the observed glands. In contrast, we regard a function of the proventricle related to feeding as more plausible. However, future experimental studies are necessary to unravel the function of the syllid proventricle.

Reproduction

Syllids show a spectacular diversity of reproductive modes and their variety of schizogamic forms are notable and unique within annelids. For the Syllinae species with scissiparity schizogamy (formation of a single stolon), gemmiparity schizogamy (formation of several stolons), and viviparity are described. Aguado et al. (2012) suggested that the kind of stolon within Syllinae contains phylogenetic information. There are five different kinds of stolons described: acephalous, acerous or *tetraglene*, dicerous or *chaetosyllis*, tetracerous, and finally, pentacerous or *ioda* (see San Martín 2003 and Aguado et al. 2012 for descriptions), and each of them is linked to a different monophyletic group (Aguado et al. 2012). *T. antoni* n. sp. produces dicerous stolons and is located within the large clade that contains all the species (for which this information is available) producing this kind of stolon. During the development of stolons, gametes are formed in the posterior segments and are then moved into the stolon segments. A similar observation has been previously reported for *Haplosyllis spongicola* (Wissocq 1966), and this process might be typical for all Syllinae.

Regeneration ability

T. antoni n. sp. exhibits high regeneration ability. Anterior regeneration is incomplete, lacking the proventricle, ventricle, caeca, and pharyngeal tooth. In contrast, regeneration of the posterior end appears to be complete. According to Okada (1929, 1938), a regeneration of the complete posterior end is common in syllids, if the section is performed after the proventricle region. When dissecting behind the proventricle, fundamental differences occur when comparing anterior and posterior regeneration. In the case of anterior regenerating individuals, the blastema is patterned during regeneration into prostomium and up to three segments. In contrast, the blastema of a posterior regenerating specimen develops only into the pygidium, and later, new segments are added possibly

by a posterior segment proliferation zone. In this case, the regenerating process seems to be coupled with the regular mechanism of growing. However, Allen (1923) also describes the existence of a growth zone during anterior regeneration in *Procerastea halleziana* Malaquin, 1893. Given that *T. antoni* n. sp. regenerates several anterior segments consecutively when dissecting in front of the proventricle, this anterior growth zone might also exist in this species, for some cases.

An incomplete regeneration of the anterior end can be also found in other syllids, including members of Autolytinae, Exogoninae, and Syllinae (e.g., Langerhans 1879; Viguier 1902; Okada 1929). Others like *Procerastea halleziana*, *Procerea picta* Ehlers, 1864, or *Syllis gracilis* Grube, 1840, are described to regenerate numerous anterior segments including the proventricle (Allen 1923; Okada 1929). Okada (1929) pointed out that in species with an incomplete anterior regeneration, only the endodermal midgut grows out anteriorly, whereas in others with complete regeneration, an ectodermal invagination occurs. The latter case makes it possible to re-develop the proventricle and the ventricle. The ability of anterior regeneration might be linked to lifestyle or asexual reproduction. For example, species with a complete anterior regeneration like *S. gracilis* or *P. halleziana* also exhibit asexual reproduction by architomic fission (Okada 1929). However, the available data is still limited to support a general pattern.

Regenerating specimens also show the development of stolons. These individuals are shorter than the usual stolonizating specimens. These individuals have neither a prostomium (for about 4 days) nor a proventricle, which could regulate this process, as previous authors suggested (Franke 1983, 1986; Heacox and Schroeder 1982). However, it cannot be ruled out that the stolonization process has been initialized prior to dissection.

The systematics of Syllinae and its future

The results of our phylogenetic analysis reveal that the division of *Typosyllis* into subgenera (*Syllis*, *Typosyllis*, and *Langerhansia*) proposed by Licher (1999) does not agree with their relationships. The simple chaetae that are a product of a fusion process of shafts and blades, a character which thought to be a synapomorphy of *Syllis* species (Licher 1999), evolved several times convergently in Syllinae (see *S. gracilis*, *S. gracilis australiensis*, and *S. ypsiloides* in Figs. 9 and 10). Additionally, other species, such as *Syllis amica* Quatrefages, 1866, and *Syllis ferrani* Alós and San Martín, 1987, may also show simple chaetae, but in these cases, by convergent loss of blades (Figs. 9 and 10).

Furthermore, other names apart from *Syllis* and *Typosyllis* were proposed though later synonymized. Such is the case of *Trichosyllis* Schmarda, 1861; *Gnathosyllis* Schmarda, 1861; *Isosyllis* Ehlers, 1864; *Pagenstecheria* Quatrefages, 1865; *Thoe* Kinberg, 1866; *Ioida* Johnston, 1840; *Aporosyllis* Quatrefages, 1865; *Chaetosyllis* Malmgren, 1867; *Langerhansia* Czerniavsky, 1881; and *Reductotyposyllis* Hartmann-Schröder 1979.

All above considered and in the light of the present phylogenetic results, the reorganization of the systematics of Syllinae is in clear need, but it is still a difficult task that needs more information to be gathered. However, we propose herein some steps to resolve this taxonomic challenge.

1. *Trypanosyllis*/*Xenosyllis*/*Eurysyllis* is well defined. Only *Trypanosyllis coeliaca* might need a new assignment considering its sister group relationship with the rest of the terminals.
2. *Branchiosyllis* and *Haplosyllis* are well defined in a supported clade. *H. spongicola* has been claimed to be a complex of species (Licher 1999; Martin et al. 2003). Molecular information may help to delimitate species within these two genera.
3. *Megasyllis*, *Paraopisthosyllis*, and a third genus not included herein, *Alcyonosyllis*, have evolved from the same ancestor and share several distinct synapomorphies.
4. *Opisthosyllis* seems to be polyphyletic. We propose to include more species since some of them might result in the same clade and maintain finally the name.
5. *Syllis*/*Typosyllis* conflict might be solved with the following recommendations. More molecular data is needed since the support values are low, and a higher taxon sampling is encouraged since most of the species within Syllinae are lacking. The type species of *Syllis* is *Syllis monilaris* Savigny, 1812 (from the Red Sea) (Lamarck 1818), whose type series is lost (Licher 1999). A neotype for *S. monilaris* (specimens from Red Sea) should be designated, and molecular information should be included in a phylogenetic study. The clade in which it will be located and its species would be named after *Syllis*. *Typosyllis* itself does not have a type species. This is because it was designated posteriorly to substitute *Syllis* as a genus, which was hence considered a subgenus. Accordingly, a type species for *Typosyllis* should be designated and we propose one of the 14 taxa included by Langerhans (1879). The clade in which it will be located and its species would be named after *Typosyllis*. Moreover, old names currently not in use should be recovered to name new clades, such as *Ioida* and *Pagenstecheria*. *Ioida* was proposed for *Ioida macrophtahalma* Johnston, 1840, by monotypy, later synonymized with *Syllis armillaris* (O.F. Muller, 1776). *Pagenstecheria* was proposed for *P. oblonga* Keferstein, 1861, by monotypy, later synonimized with *Syllis variegata* Grube, 1860. *Ioida* is currently in use to designate one kind of pentacerous sylline stolons found in *Syllis hyalina* Grube, 1863, *S. gracilis*, and *S. armillaris*.

For clades that are well supported and different to the ones already mentioned, new names should be proposed.

6. Inclusion of species representing other Syllinae genera, such as *Dentatisyllis*, *Inermosyllis*, *Karroonsyllis*, *Nuchalosyllis*, *Parasphaerosyllis*, *Plakosyllis*, *Rhopalosyllis*, and *Tetrapalpia*. Considering their morphological features and previous results (Aguado and San Martín 2009), *Nuchalosyllis* and *Plakosyllis* might be related to *Trypanosyllis*/*Eurysyllis*/*Xenosyllis* clade. In addition, there are still 19 more genera of other subfamilies that have not been included in any previous molecular phylogenetic study (Aguado et al. 2012). Their relationships with the rest of syllids have still to be studied in more detail.

Outlook

The reproduction of syllids bears several evolutionary interesting phenomena, but only few studies tackled the molecular, morphological, or behavioral background to understand the unique modes in this group of annelids. The taxonomic complexity as well as lack of established lab cultures seems to have hampered detailed studies regarding these questions. *T. antoni* n. sp. and putatively related species of the *Syllis*/*Typosyllis* complex are well suited to address such questions. We provide a solid phylogenetic background for this species, a pre-requisite for any type of evolutionary study. Moreover, we give a detailed description of the morphology and describe the regeneration process. Several future research questions should be addressed: Is there a common molecular basis for regeneration and development; are the same genes involved in stolonization and regeneration; what molecular changes are needed to evolve gemmiparity from scissiparity; and what makes an animal growing branches as reported for *Ramisyllis*? We hope that the here presented results stimulate interest in evolutionary research of syllids.

Acknowledgments We are very grateful to Pat Hutchings, Anna Murray, and Stephen Keable (AM) for the kind loan of specimens; Angelika Brandt, Kathrin Philipps, and Petra Wagner (ZMH) for the loan of *T. heronislandensis* paratypes; Javier Sánchez (MNCN) for providing us with catalogue numbers for *Typosyllis antoni* n. sp.; Alberto García (MNCN) for his help with SEM process; and Maher Fahim (UAM) for his help with pictures at the light microscopy. We are very grateful to Miguel Angel Alonso Zarazaga (MNCN) for sharing his expertise, fruitful discussions, and all his kind help investigating into the nomenclature conflicts around the genera *Syllis* and *Typosyllis*. This study has been partly supported by a Geddes visiting fellowship to MTA for a research stay at the Australian Museum. CH and MW were supported by special funds of the University of Leipzig. CB received funding from the DFG (BL787/5-1).

References

Aguado, M. T., & San Martín, G. (2006). Sílidos intersticiales (Syllidae: Polychaeta) del Parque Nacional de Coiba (Pacífico, Panamá). *Revista de Biología Tropical, 54*(3), 725–743.

Aguado, M. T., & San Martín, G. (2009). Phylogeny of the Syllidae (Polychaeta) based on morphological data. *Zoologica Scripta, 38*, 379–402.

Aguado, M.T; San Martín, G., & Nishi, E. (2006). Two new species of Syllidae (Annelida: Polychaeta) from Japan. *Scientia Marina, 70S3,* 9–16.

Aguado, M. T., Nygren, A., & Siddall, M. E. (2007). Phylogeny of Syllidae (Polychaeta) based on combined molecular analysis of nuclear and mitochondrial genes. *Cladistics, 23*, 552–564.

Aguado, M. T., San Martín, G., & Ten Hove, H. (2008). Syllidae (Annelida: Polychaeta) from Indonesia collected in the Siboga (1899–1900) and Snellius II (1984) expeditions. *Zootaxa, 1673*, 1–48.

Aguado, M. T., San Martín, G., & Siddall, M. (2012). Systematics and Evolution of syllids (Annelida, Syllidae). *Cladistics, 28*, 234–250.

Allen, E. J. (1923). Regeneration and reproduction of the syllid *Procerastea. Philosophical Transactions of the Royal Society, London, B., 211*, 131–177.

del Castillo, J., Anderson, M., & Smith, D. S. (1972). Proventriculus of a marine annelid: muscle preparation with the longest recoded sarcomere. *Proceedings of the National Academy of Sciences, USA, 69*(7), 1669–1672.

Farris, J., Abert, V., Källersjö, M., Lipscomb, D., & Kluge, A. (1996). Parsimony jackknifing outperforms neighbor-joining. *Cladistics, 12*, 99–124.

Fauchald, K., & Jumars, P. A. (1979). The diet of worms: a study of polychaete feeding guilds. *Oceanography and Marine Biology, 17*, 193–284.

Filippova, A., Purschke, G., Tzetlin, A. B., & Müller, M. C. M. (2010). Musculature in polychaetes: comparison of *Myrianida prolifera* (Syllidae) and *Sphaerodoropsis* sp. (Sphaerodoridae). *Invertebrates Biology, 129*, 184–198.

Fischer, A., & Dorresteijn, A. (2004). The polychaete *Platynereis dumerilii* (Annelida): a laboratory animal with spiralian cleavage, lifelong segment proliferation and a mixed benthic/pelagic life cycle. *BioEssays, 26*, 314–325.

Fischer, A., & Fischer, U. (1995). On the life-style and life-cycle of the luminescent polychaete *Odontosyllis enopla* (Annelida: Polychaeta). *Invertebrate Biology, 114*, 236–247.

Franke, H. D. (1983). Endocrine mechanisms mediating light-temperature effects on male reproductive activity in *Typosyllis prolifera* (Polychaeta, Syllidae). *Wilhelm Roux's Archives of Developmental Biology, 192*, 95–102.

Franke, H. D. (1986). The role of light and endogenous factors in the timing of the reproductive cycle of *Typosyllis prolifera* and some other polychaetes. *American Zoologist, 26*, 433–445.

Franke, H. D. (1999). Reproduction of the Syllidae. *Hydrobiologia, 402*, 39–55.

Glasby, C. J. (2000). *Family Syllidae* (In Beesley, P.L., Ross, G.J.B., & Glasby, C.J. (Eds.), *Polychaetes and allies*: *The Southern Synthesis. Fauna of Australia. Vol. 4 Polychaeta*, *Myzostomida*, *Pogonophora*, *Echiura*, *Sipuncula* (pp. 161–167)). Melbourne: CSIRO Publishing.

Glasby, C. J., Schroeder, P. C., & Aguado, M. T. (2012). Branching out: a remarkable new branching syllid (Annelida) living in a *Petrosia* sponge (Porifera: Demospongiae). *Zoological Journal of the Linnean Society, 164*, 481–497.

Goloboff, P. A., Farris, J. S., & Nixon, K. (2008). TNT: a free program for Phylogenetic analysis. *Cladistics, 24*, 774–786.

Hartmann-Schröder, G. (1979). Teil 2. Die Polychaeten der tropischen Nordwestküste Australiens (zwischen Port Samson in Norden und

Port Hedland in Süden). Zur Kenntnis des Eulitorals der australischen Küsten, unter besonderer Berücksichtigung der Polychaeten und Ostracoden. *Mitteilungen aus dem hamburgischen zoologischen Museum und Institut*, *76*, 75–218.

Hartmann-Schröder, G. (1981). Teil 6. Die Polychaeten der tropisch-subtropischen Westküste Australiens (zwischen Exmouth im Norden und Cervantes im Süden). *Mitteilungen aus dem hamburgischen zoologischen Museum und Institut*, *78*, 19–96.

Hartmann-Schröder, G. (1989). Teil 14. Die Polychaeten der antiborealen und subtropisch-tropischen Küste Südost-Australiens zwischen Lakes Entrance (Victoria) im Süden und Maclean (New South Wales) im Norden. *Mitteilungen aus dem hamburgischen zoologischen Museum und Institut*, *86*, 11–63.

Hartmann-Schröder, G. (1991). Teil 16. Die Polychaeten der subtropisch-tropischen bis tropischen Ostküste Australiens zwischen Maclean (New South Wales) und Gladstone (Queensland) sowie von Heron Island (Grosses Barriere-Riff). *Mitteilungen aus dem hamburgischen zoologischen Museum und Institut*, *88*, 17–71.

Haswell, W. A. (1920). Australian Syllidae, Eusyllidae and Autolytidae. *Journal of the Linnean Society of London, 24*, 90–112.

Heacox, A. E., & Schroeder, P. (1982). The effects of prostomium and proventriculus removal on sex determination and gametogenesis in *Typosyllis pulchra* (Polychaeta: Syllidae). *Wilhelm Roux's Archives of Developmental Biology, 191*, 84–90.

Helm, C., Weigert, A., Mayer, G., & Bleidorn, C. (2013). Myoanatomy of *Myzostoma cirriferum* (Annelida, Myzostomida): implications for the evolution of the myzostomid body plan. *Journal of Morphology, 274*, 456–466.

Jeuniaux, C. (1969). Nutrition and digestion. In M. Florkin & B. T. Scheer (Eds.), *Chemical Zoology* (Annelida, Echiura, and Sipuncula, Vol. IV, pp. 69–91). New York: Academic.

Katoh, K., Misawa, K., Kuma, K., & Miyata, T. (2002). MAFFT: a novel method for rapid multiple sequence alignment based on fast Fourier transform. *Nucleic Acids Research, 30*, 3059–3066.

Lamarck, J. B. P. A. D. (1818). *Histoire Naturelle des animaux sans vertèbres, présentant les caractères generaux et particuliers de ces animaux, leur distribution, leur classes, leur familles, leur genres, et la citation synonymique des principales espèces qui s´y rapportent; précedés d'une introduction offrant la détermination des caractères essentiels de l'Animal, sa distinction du végétal et des autres corps naturelles, enfin l'Exposition des Principes fondamentaux de la Zoologie* (Vol. 5). Paris: Deterville. 612pp.

Langerhans, P. (1879). Die Würmfauna van Madeira. *Zeitschrift für Wissenschaftliche Zoologie, 33*, 513–592.

Licher, F. (1999). Revision der Gattung *Typosyllis* Langerhans, 1879 (Polychaeta: Syllidae). Morphologie, taxonomie und phylogenie. *Abhandlungen der Senckenbergischen Naturforschenden Gesellschaft*, *551*, 1–336.

Nygren, A. (1999). Phylogeny and reproduction in Syllidae (Polychaeta). *Zoological Journal of the Linnean Society, 126*, 365–386.

Martin, D., Temir, A. B., San Martín, G., & Gil, J. (2003). Inter-population variability and character description in the sponge-associated *Haplosyllis spongicola* complex (Polychaeta: Syllidae). *Hydrobiologia, 496*, 145–162.

Okada, Y. K. (1929). Regeneration and fragmentation in the syllidian polychaetes. *Wilhelm Roux' Archiv für Entwicklungsmechanik der Organismen, 115*, 542–600.

Okada, Y. K. (1938). An internal factor controlling posterior regeneration in syllid polychaetes. *Journal of the Marine Biological Association of the United Kingdom, 23*, 75–78.

Pleijel, F. (2001). *Syllidae, Grube, 1850* (In Rouse, G.W., & Pleijel, F. (Eds.), *Polychaetes* (pp. 102–105)). New York: Oxford University Press.

Purschke, G., & Müller, M. C. M. (2006). Evolution of body wall musculature. *Integrative and Comparative Biology, 46*, 497–507.

San Martín, G. (1984). Estudio biogegráfico, faunístico y sistemático de los Poliquetos de la familia Sílidos (Syllidae: Polychaeta) en Baleares. *Ediciones de la Universidad Complutense de Madrid, 187*, 529.

San Martín, G. (2003). Annelida, Polychaeta II: Syllidae. In Ramos, M.A. et al. (Eds.), *Fauna Ibérica*, vol. 21. Museo Nacional de Ciencias Naturales. CSIC. Madrid, 554pp.

Simakov, O., Larsson, T. A., & Arendt, D. (2013). Linking micro- and macro-evolution at the cell type level: a view from the lophotrochozoan *Platynereis dumerilii*. *Briefings in Functional Genomics, 12*, 430–439.

Stamatakis, A. (2006). RAxML-VI-HPC: maximum likelihood-based phylogenetic analyses with thousands of taxa and mixed models. *Bioinformatics, 22*, 2688–2690.

Stamatakis, A., Hoover, P., & Rougemont, J. (2008). A rapid bootstrap algorithm for the RAxML Web servers. *Systematic Biology, 57*, 758–771.

Storch, V. (1968). Zur vergleichenden Anatomie der segmentalen Muskelsysteme und zur Verwandtschaft der Polychaeten-Familien. *Zeitschrift für Morphologie der Tiere, 63*, 251–342.

Tzetlin, A. B., & Filippova, A. V. (2005). Muscular system in polychaetes (Annelida). *Hydrobiologia, 535*(536), 113–126.

Viguier, C. (1902). Sur la valeur morphologique de la tête des Annélides. *Annales Des Sciences Naturelles (Zoologie), 25*, 281–293.

Weigert, A., Helm, C., Meyer, M., Nickel, B., Arendt, D., Hausdorf, B., Santos, S. R., Halanych, K. M., Purschke, G., Bleidorn, C., & Struck, T. H. (2014). Illuminating the base of the annelid tree using transcriptomics. *Molecular Biology and Evolution, 31*, 1391–1401.

Westheide, W. (1974). Interstitielle Fauna von Galapagos. XI. Pisionidae, Pilargidae, Syllidae. *Mikrofauna Meeresbodens, 44*, 195–338.

Wissocq, J. C. (1966). La sexualisation du stolon chez *Syllis spongicola* Grübe. *Cahiers de Biologie Marine, 7*, 337–342.

Zantke, J., Bannister, S., Rajan, V. B. V., Raible, F., & Tessmar-Raible, K. (2014). Genetic and genomic tools for the marine annelid *Platynereis dumerilii*. *Genetics, 197*, 19–31.